Genomics 112 (2020) 2130–2145

Contents lists available at ScienceDirect

Genomics

journal homepage: www.elsevier.com/locate/ygeno

Original Article

Dual RNA-Seq analysis of *Medicago truncatula* and the pea powdery mildew *Erysiphe pisi* uncovers distinct host transcriptional signatures during incompatible and compatible interactions and pathogen effector candidates

Megha Gupta[a,c,1], Gunjan Sharma[a,1], Divya Saxena[a,2], Roli Budhwar[b], Madavan Vasudevan[b], Varsha Gupta[a], Arunima Gupta[a], Rashi Gupta[a], Divya Chandran[a,*]

[a] Laboratory of Plant-Microbe Interactions, Regional Centre for Biotechnology, NCR Biotech Science Cluster, Faridabad 121001, India
[b] Bionivid Technology Pvt. Ltd., Kasturi Nagar, Bangalore, India
[c] Kalinga Institute of Industrial Technology, Bhubaneswar, India

ARTICLE INFO

Keywords:
Obligate biotroph
MtREP1
Dual transcriptome
TCP
Growth-defense tradeoff
Egh16H

ABSTRACT

Powdery mildew (PM) is a serious fungal disease of legumes. To gain novel insights into PM pathogenesis and host resistance/susceptibility, we used dual RNA-Seq to simultaneously capture host and pathogen transcriptomes at 1 d post-inoculation of resistant and susceptible *Medicago truncatula* genotypes with the PM *Erysiphe pisi* (*Ep*). Differential expression analysis indicates that *R*-gene mediated resistance against *Ep* involves extensive transcriptional reprogramming. Functional enrichment of differentially expressed host genes and in silico analysis of co-regulated promoters suggests that amplification of PTI, activation of the JA/ET signaling network, and regulation of growth-defense balance correlate with resistance. In contrast, processes that favor biotrophy, including suppression of defense signaling and programmed cell death, and weaker cell wall defenses are important susceptibility factors. Lastly, *Ep* effector candidates and genes with known/putative virulence functions were identified, representing a valuable resource that can be leveraged to improve our understanding of legume-PM interactions.

1. Introduction

Powdery mildew fungi are obligate biotrophic pathogens that infect a wide variety of crops, including legumes [1], which represent a major component of food crops consumed worldwide. The disease causes significant yield losses in several legumes such as pea [2], lentils [3] and mung bean [4]. The most widely documented powdery mildew (PM) on pea is *Erysiphe pisi* (*Ep*), which, like other PMs, exclusively infects the host epidermal cell with well-defined stages of infection [5]. Early infection stages include germination of the conidia (1–2 h post-inoculation (hpi)), multi-lobed appressorium formation (3–6 hpi), epidermal cell penetration (6–18 hpi), and development of the primary haustorium, the feeding structure (by 24 hpi). Later infection stages include the formation of surficial mycelial networks and secondary haustoria followed by asexual reproduction at 5 days post-inoculation (dpi). Being an obligate biotroph, the fungus modulates cellular architecture and metabolism of living host cells to divert nutrients for its growth and reproduction while limiting host defense responses, including cell death [6].

Investigations into the genetic and molecular mechanisms of PM resistance have primarily focused on the model dicot *Arabidopsis* and monocots, barley and wheat. These studies have demonstrated that plants have evolved multiple, distinct, and often host-specific strategies to counter the pathogen [7–13]. In contrast, mechanisms of PM resistance in legumes are relatively underexplored. To date, only two recessive (*er1* and *er2*) and one dominant (*Er3*) genes with a role in PM resistance have been characterized in pea [2]. Although *er1* is extensively used in breeding programs, the durability of resistance is of concern since a breakdown in resistance via pathogen counter-evolution has already been reported [14]. Therefore, there is a need to identify new sources of resistance to PM in pea. The diploid legume *Medicago truncatula* (*Mt*, barrel medic) is a valuable resource for

* Corresponding author at: Laboratory of Plant-Microbe Interactions, Regional Centre for Biotechnology, NCR Biotech Science Cluster, 3rd Milestone, Faridabad-Gurgaon Expressway, Faridabad 121001, Haryana, India.
E-mail address: divya.chandran@rcb.res.in (D. Chandran).
[1] These authors have contributed equally to this work.
[2] Present address: School of Computational and Integrative Sciences, Jawaharlal Nehru University, New Delhi, India.

https://doi.org/10.1016/j.ygeno.2019.12.007
Received 3 September 2019; Received in revised form 14 November 2019; Accepted 9 December 2019
Available online 16 December 2019
0888-7543/

investigating the molecular mechanisms governing various aspects of legume biology [15] since it has all the attributes of a model plant, including a sequenced genome [16]. Incidentally, *Ep* can infect *Mt*, and accessions with varying degrees of susceptibility have been used to identify new sources of PM resistance. So far, two resistance QTLs [17], and a dominant resistance gene (*MtREP1*) have been identified [18]; however, the molecular mechanisms of resistance have not yet been uncovered.

Pathogen recognition is an important aspect of plant immunity and is mediated by cell surface pattern-recognition receptors (PRRs) and intracellular nucleotide-binding domain LRR-domain containing receptor (NLR or R) proteins. Receptor-like kinases (RLKs) function as PRRs, which recognize diverse pathogen-associated molecular patterns (PAMPs) or damage-associated molecular patterns (DAMPs) to initiate PAMP-triggered immunity (PTI) [19,20]. To suppress PTI and promote infection, pathogens secrete virulence proteins termed effectors into host cells [21], which leads to effector-triggered susceptibility. However, some of these effectors are recognized either directly or indirectly by host R proteins, resulting in effector-triggered immunity (ETI) [22,23]. Since effectors play key roles in determining the outcome of plant-pathogen interactions their identification is equally integral to improving our understanding of the disease. The genome sequence of *Ep* is currently available as a draft assembly of 69.26 Mbp [24]. This resource combined with expression analysis can provide insights into the pathogenicity determinants in this species. This has been demonstrated for PMs such as *Blumeria graminis* f.sp. *hordei* (*Bgh*) [25], *Golovinomyces orontii* [26], *Erysiphe necator* [27], *Podosphaera xanthii* [28], and more recently for *Ep* [29].

Genome-wide gene expression profiling presents a global view of the genes and functional pathways that are impacted during disease development and has been successfully used to obtain valuable insights into the molecular mechanisms of resistance. Transcriptomic studies were previously performed on the *Mt-Ep* pathosystem using different combinations of pathogen isolates and host genotypes and different microarray platforms [30–32]. However, these studies only profiled changes in host gene expression, and except for one 16 K oligo array study, were all performed on cDNA arrays spotted with limited sets of user-selected genes (1 or 6 K arrays). We posit that the limited number of genes profiled in these studies combined with the incomplete annotation of the *Mt* genome available at the time would have prevented the capture of comprehensive, genome-wide changes in gene expression during *Ep* infection. RNA-Seq has recently emerged as a powerful tool to study global changes in expression during host-pathogen interactions as it provides an unbiased, discovery-based expression profiling that is more sensitive than microarrays. Further, it can be used to simultaneously capture host and pathogen transcriptomes, a technique commonly referred to as 'Dual RNA-Seq' [33]. This method has been successfully used to gain novel biological insights into diverse plant-pathogen interactions [34–37].

To obtain new insights into the *Ep-Mt* interaction, we generated dual RNA-Seq transcriptomic data during an early stage of *Ep* infection (1 dpi) in resistant and susceptible *Mt* genotypes. We identified differential host transcriptional changes associated with incompatibility and compatibility, which allowed us to uncover novel processes and components of the *Ep–Mt* interaction. We also identified infection-altered transcription factors and enriched *cis*-acting regulatory elements in co-regulated promoters, which enabled us to identify putative regulators underlying resistance and susceptibility. Lastly, we exploited the dual transcriptome to predict novel *Ep* effector candidates and discuss their potential roles as virulence factors.

2. Materials and methods

2.1. Plant growth, PM infection, and microscopy

Seeds of *Mt* genotypes A17 (resistant) and DZA315.16 (susceptible) were grown and infected with a moderate inoculum of *Ep* isolate Palampur-1 [38] as per [39]. To minimize plant-to-plant variation, 6 evenly spaced plants were grown within each box using a design that alternates the placement of A17 and DZA. At 3.5 weeks, a subset of protrays was infected with a moderate inoculum of *Ep* (conidia from one and a half fully infected AzadP-3 pea leaves at 10–14 dpi per protray) using a settling tower and mesh screen [39]. This method of inoculation was used to enhance reproducibility from experiment to experiment and minimize plant-to-plant variation. Two independent biological replicate experiments were performed. From each experiment, five fully expanded mature trifoliate leaves were harvested per genotype from a total of five non-inoculated and five inoculated plants at 1 dpi, immediately frozen in liquid nitrogen and stored at −80 °C before RNA extraction. Two additional trifoliate leaves were harvested from two inoculated plants of each genotype for microscopic analysis of pathogen growth stages. To visualize fungal growth, infected leaves were stained with trypan blue [40] and viewed under bright field using a Zeiss PALM MicroBeam microscope. For *in planta* expression analysis of candidate fungal effectors, three-week-old DZA plants were inoculated with *Ep* conidia using a brush. Infected leaf tissues (one trifoliate leaf each, from three independent biological replicates) were harvested at 0, 6, 12, 24, 48, 72, and 120 hpi, immediately frozen in liquid nitrogen and stored at −80 °C until RNA extraction.

2.2. RNA isolation, library construction, and Illumina sequencing

For each RNA-Seq sample, total RNA was isolated from 5 trifoliate leaves using TRIzol® reagent (ThermoFisher Scientific) and treated with DNase I (NEB) to remove genomic DNA contamination. RNA quantity and quality was measured using an Agilent 2100 Bioanalyzer followed by ribosomal RNA depletion using the Ribominus plant kit (Invitrogen). Libraries were prepared from 150 ng rRNA-depleted RNA using the Illumina TruSeq RNA Sample Preparation Kit v2 and sequenced using Illumina HiSeq 2500 in 100 bp paired-end mode. For *in planta* expression analysis of candidate fungal effectors, total RNA was extracted from frozen leaf samples using the Nucleospin RNA Plant kit (Macherey-Nagel) with on-column DNase treatment.

2.3. Genome-guided de novo transcriptome assembly

Paired-end raw reads in FASTQ format were subjected to quality control using the NGS QC toolkit v2.3.3 [41]. Since the *Mt* genome has gaps in the assembly along with unanchored scaffolds [16], and the available *Ep* genome is at scaffold level, we used genome-guided *de novo* transcriptome assembly to capture the sequence variations contained in our RNA-Seq samples in the form of transcripts that are *de novo* reconstructed. High quality (HQ) paired-end replicate libraries of all four samples (A17 control, A17 inoculated, DZA control, DZA inoculated) were mapped against the merged *Mt* A17 reference genome (https://www.ncbi.nlm.nih.gov/genome/?term=Medicago) and *Ep* scaffolds (https://www.mpipz.mpg.de/23693/Powdery_Mildews) using TopHat v2.0.11 (parameters: -r 150-mate-std-dev 50) [42]. Genome-guided *de novo* assembly was performed using a De bruijn graph-based 'Trinityrnaseq-2.0.6' Assembler [43]. Assembled transcripts with length > 200 bp were ameliorated with average depth ≥ 5 and coverage ≥70% using an in-house script [44]. 100% identical transcripts were removed using CD-HIT-EST to generate a set of non-redundant transcripts. The final assembly was evaluated by mapping HQ paired-end reads to non-redundant transcripts using RSEM [45]. The expression levels of transcripts in the individual libraries were assessed by mapping the HQ reads to the assembled transcriptome using Bowtie 2 [46]. The Principal Component Analysis (PCA) plot was constructed using Scatterplot3d package in R software [47].

2.4. Segregation and annotation of host and pathogen transcripts

To segregate host and pathogen transcripts from the mixed transcriptome, blastn alignments were performed against the *Mt* reference genome (query coverage ≥95%; e-value ≤1e-05) and *Ep* scaffolds (query coverage ≥90%; e-value ≤1e-05). Transcripts that aligned to both genomes were removed from further analysis. Host transcripts were annotated by performing blastx alignments against the *Mt*4.0v2 protein database (http://www.medicagogenome.org/) and plant Refseq protein database (July 2018 release; NCBI) using query coverage ≥50% and e-value ≤1e-03 as the cut-off. [48]. From the set of annotated transcripts, the longest unique ones were retained. Fungal transcripts that were represented by reads only in inoculated samples or < 10 reads in uninoculated control samples were retained. Further, since the available *Ep* reference genome assembly is highly fragmented, sequences that did not align to either genome or have a plant annotation, but were represented by reads only in the inoculated samples (or < 10 reads in control samples) were added to the list of putative fungal transcripts. For annotation of fungal transcripts, blastx alignments were performed on *E. necator* and *Bgh* protein databases (ftp://ftp.ensemblgenomes.org/pub/fungi), *G. orontii* haustorial protein database [26], and Ascomycete and fungal nr protein databases (NCBI). Query coverage ≥50% and e-value ≤1e-03 was applied, and the best hit was retained.

2.5. Analysis and functional enrichment of Mt DEGs and Ep genes

Differentially expressed genes (DEGs) between the groups were calculated by the DESeq2 package in R version 3.2.5 [49]. The threshold for DEGs was set as $|\log_2$ fold-change$| \geq 1.0$ and ≤ -1.0 and *p*-value ≤.05. We computed both p-value and p-adjusted value as a part of our standard analysis. To estimate the degree of biological variation between replicates and to identify differentially expressed transcripts with acceptable false discovery rate (FDR), we proceeded with p-value as FDR to measure the total number of biologically meaningful DEGs [50]. MedicMine (http://medicmine.jcvi.org/medicmine/begin.do) and MapMan [51] were used to identify significantly enriched gene ontology (GO) terms and pathways in the DEG datasets. REVIGO was used to remove redundant GO terms, and the resulting non-redundant terms were visualized in semantic similarity-based scatterplots [52]. Enriched cis-acting regulatory elements were identified in 1-kb upstream promoter sequences of DEGs using the 'Regulation Prediction' tool in PlantRegMap (v4.0) [53], and motif names were obtained from the plant cis-acting regulatory element (PLACE) database [54]. *Mt* transcription factors were identified from the DEG datasets using PlantTFDB [53]. GO terms and InterPro domain information was obtained for the fungal genes via BLAST2GO [55]. Open reading frames (ORFs) were predicted for fungal transcripts using TransDecoder [43] with a minimum peptide length of 50 amino acids. Protein domains were predicted using HMMER v3.2 with Pfam 31.0 database.

2.6. Ep candidate effector prediction

ORFs containing genuine start codons were used for the prediction of candidate effectors. Signal peptides (SP) were predicted using SignalP3.0 and SignalP4.1 (D-score cut-off value ≥0.5) [56,57] and subcellular localization was predicted using TargetP1.1 [58]. Proteins with SP and predicted location "S" (secretory) were retained. The presence of transmembrane (TM) domain(s) was predicted by the TMHMM2.0 server [59] and proteins having no TM or TM within the SP were retained. Lastly, proteins predicted to have a GPI modification site via Big-Pi fungal predictor [60] were removed. ApoplastP was used to predict localization of effector proteins to the plant apoplast [61]. Localizer was used to predict subcellular localization of effector proteins in the plant cell [62].

2.7. Quantitative real-time PCR (qPCR) validation

First-strand cDNA was synthesized from 1 μg DNase I-treated total RNA using iScript™ cDNA Synthesis Kit (Bio-Rad) according to the manufacturer's instructions. qPCR was performed on cDNA samples using either 5× HOT FIREPol® EvaGreen® qPCR mix (Solis Bio dyne) or SYBR Premix Ex Taq II (TaKaRa) in a QuantStudio Flex 6 ABI system (ThermoFisher Scientific) according to the manufacturer's instructions. For quantification of *MtPR10* and *MtREP1*, *Mt ubiquitin* (*MtUBQ; Medtr3g092130*) served as the reference gene and fold change was calculated using LinRegPCR (v2015.1; [63]). Estimation of the relative abundance of plant and fungal RNA in the infected samples was performed via qPCR analysis of specific *Mt* (AF233339.1) and *Ep* (AF02842.1) internal transcribed spacer (ITS) sequences [64]. *MtUBQ* served as the reference gene and relative expression was calculated using LinRegPCR. For qPCR validation of plant and fungal genes, *MtUBQ and Ep β-tubulin 2* (*Eptub2;* X81961.1) served as the reference genes, respectively, and $\log_2$ fold change values were calculated using the comparative C_T method [65]. Three technical replicates from three independent biological replicates were processed for each sample. Primers were designed using the NCBI Primer BLAST tool (Supplementary Table S1). Correlation analysis between RNA-Seq and qPCR expression values was performed using Graphpad Prism (v7.02).

3. Results

3.1. Quantification of Ep growth on Mt genotypes and RNA-Seq

The *Mt* genotype A17 was previously reported to display complete resistance to various isolates of *Ep* whereas DZA was reported to be highly susceptible [17,30]. To test the virulence of the *Ep* isolate Palampur-1, we assessed fungal growth on leaf tissues of both genotypes over the course of infection. In agreement with previous studies, we found that A17 was highly resistant to *Ep* Palampur-1 with no visible macroscopic disease symptoms at 12 dpi. The majority of the conidia were arrested at the multi-lobed appressorium stage by 1 dpi (Fig. 1A), and at 3 and 5 dpi, infected epidermal cells showed symptoms of hypersensitive response (HR)-like cell death, including cytoplasmic disorganization and browning [66,67]. Likewise, DZA was highly susceptible to the isolate; infected leaves were completely covered with white powder by 12 dpi. Microscopic evaluation of infected DZA leaves revealed that multi-lobed appressoria and primary hyphae were formed by 1 dpi, extensive surficial hyphae by 3 dpi and asexual reproductive structures (conidiophores) by 5 dpi (Fig. 1A).

To capture differential host responses associated with resistance/susceptibility and identify novel *Ep* effector candidates, we used RNA-Seq to simultaneously profile host and pathogen transcripts using RNA extracted from A17 and DZA leaves harvested at 1 dpi with (inoculated) or without (non-inoculated control) *Ep* challenge. We selected 1 dpi for the transcriptome analysis in order to detect *Mt* and *Ep* genes regulated prior to the appearance of visible HR symptoms in A17 and also those regulated after primary haustorium (infection/feeding structure) is fully formed in DZA. Prior to RNA-Seq, we ascertained the extent of *Ep* colonization in the samples via quantification of fungal growth stages (Fig. 1B). In A17, 0.3% of the conidia formed multi-lobed appressoria and primary hyphae, 69% formed only multi-lobed appressoria, and 31% did not germinate. In contrast, the extent of fungal colonization was greater in DZA; 51% of the conidia formed multi-lobed appressoria and primary hyphae, 41% formed only appressoria, and 8% did not germinate. This result was supported by qPCR analysis of *Mt* and *Ep* internal transcribed spacer (ITS) sequences, which indicated that the proportion of fungal biomass in the harvested leaf tissues of DZA was ~2.7-fold greater than in A17 (Fig. 1C). To validate the infection status of the samples, we quantified the transcript abundance of a plant defense marker, *PR10*. *MtPR10* was induced ~160-fold in A17 and ~15-fold in DZA (Fig. 1D), implying that although defense responses were

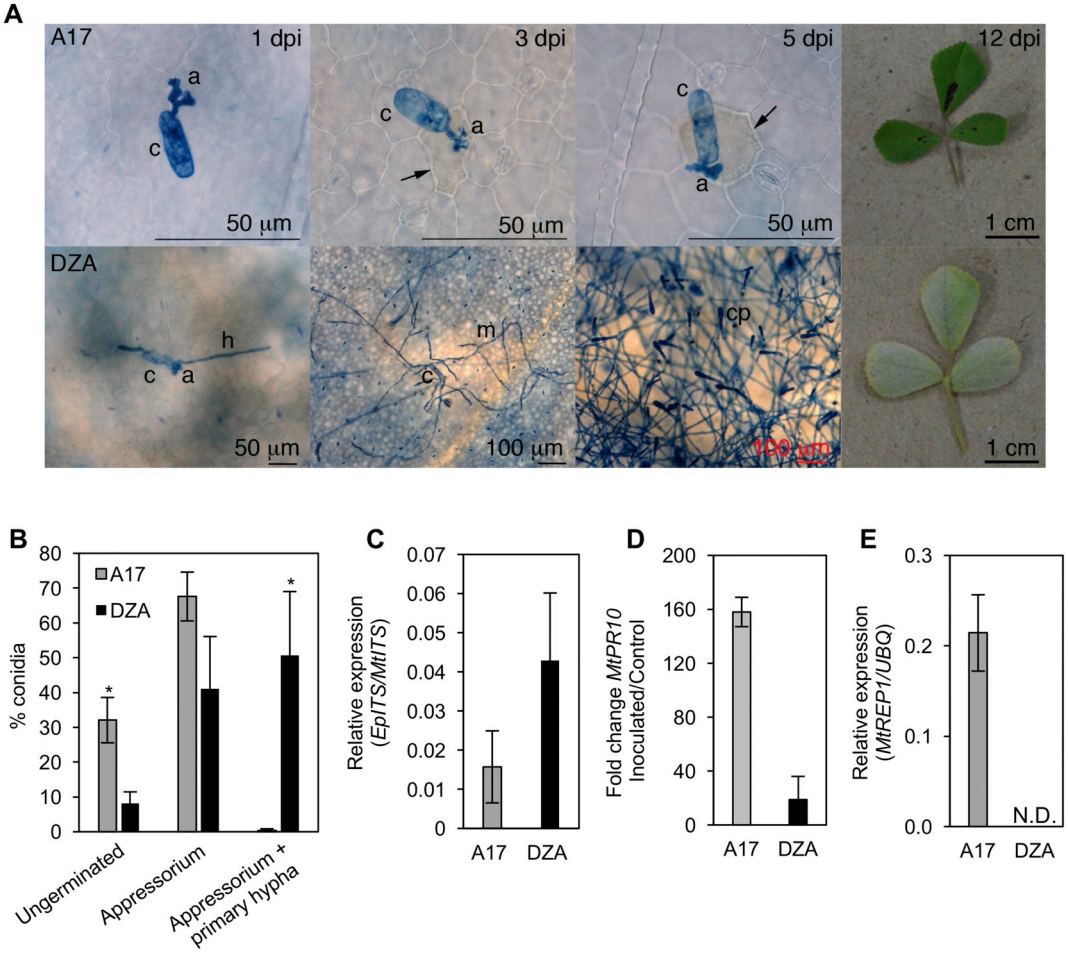

Fig. 1. Powdery mildew disease progression and *Ep* quantification on resistant (A17) and susceptible (DZA) *Mt* genotypes. (A) Trypan blue stained images of *Ep* isolate Palampur-1 on A17 and DZA leaves at 1, 3 and 5 days' post inoculation (dpi) with an image of representative leaves at 12 dpi. c, conidia; a, appressorium; h, primary hypha; m, mycelium; cp, conidiophores. Arrows point to infected epidermal cells showing cytoplasmic disorganization and browning (B) The percent of *Ep* conidia that reached different developmental stages (i.e. ungerminated, formed an appressorium or formed a colony with primary hypha) at 1 dpi assessed from > 250 conidia from 5 to 6 leaves per genotype. Asterisk indicates values that are significantly different ($^*p < .05$ based on Student's *t*-test) between A17 and DZA at the respective growth stage. (C) Relative abundance of fungal and plant ribosomal RNA in samples determined by qPCR of *Ep* ITS relative to *Mt* ITS. (D) Expression of *MtPR10* in response to *Ep*. *MtUBQ* served as the endogenous control. (E) Basal expression levels of *MtREP1* in A17 and DZA non-inoculated plants; N.D., not determined. Data shown are averages ± SD of two independent biological replicates. (For interpretation of the references to colour in this figure legend, the reader is referred to the web version of this article.)

activated in both genotypes, they were activated to a greater magnitude during the incompatible interaction. Since *MtREP1* was previously identified as one of the *R* genes responsible for PM resistance in A17 [18], we checked whether the observed differences in PM phenotypes of A17 and DZA correlated with differences in basal expression of *MtREP1*. *MtREP1* was constitutively expressed in uninoculated A17 samples whereas no transcripts were detected in DZA (Fig. 1E).

Keeping in mind the low relative abundance of fungal RNA in the mixed RNA samples (Fig. 1C), we performed deep RNA-Seq on control and *Ep*-inoculated replicate cDNA libraries of A17 and DZA and generated an average of 95 million HQ paired-end reads per sample (Supplementary Table S2). Across sample and within replicate variation in sequencing depth was < 20% indicating uniformity in data generation, which is a critical requirement for estimation of transcript coverage and normalization. The bioinformatics pipeline used for data analysis is outlined in Supplementary Fig. S1.

3.2. Assembly of the dual transcriptome and segregation of host and pathogen transcripts

Genome-guided *de novo* transcriptome assembly yielded a total of 42,302 transcripts across the four conditions profiled, totaling to an average transcriptome size of ~42 Mb (Supplementary Table S3). The average transcript length was ~1 kb and the average N50 contig length was ~1.5 kb. Expression profiling of the transcriptome identified an average of ~30,000 transcripts with baseline expression in each of the four conditions (Supplementary Fig. S2). An investigation into replicate reproducibility by PCA and unsupervised hierarchical clustering revealed a high degree of correlation between biological replicates (Supplementary Fig. S3). Collectively, these results suggest that the assembled transcriptome is highly reliable and a true reflection of positive measurement.

Based on blastn and blastx alignments, we designated 28,904 (99.2%) transcripts of the dual transcriptome as belonging to the host (*Mt*) and 140 (0.5%) as belonging to the pathogen (*Ep*) (Supplementary Table S4; see Materials and Methods for details). Blastx analysis revealed that 67% of the host transcripts show similarities to *Mt* and/or plant Refseq proteins (Supplementary Datasheet S1). Similarly, 72.4% of the pathogen transcripts are associated with at least one annotation, of which 67.4% show sequence similarities to Ascomycete proteins and 46.7% show sequence similarities to *E. necator* proteins (Supplementary Table S5). To validate the segregated transcripts, we analyzed sample-

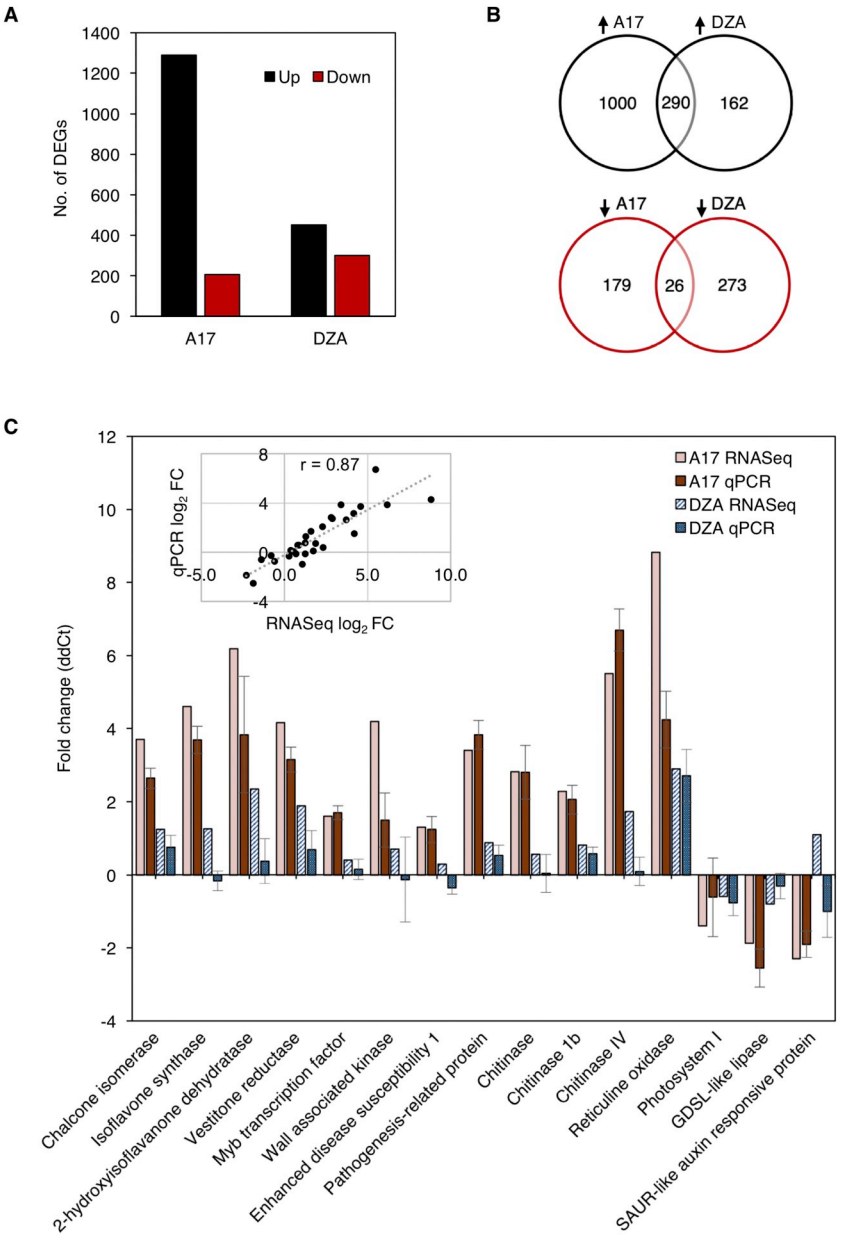

Fig. 2. Differential expression analysis of host genes upon *Ep* inoculation. (A) Number of differentially expressed genes (DEGs) in 1 dpi versus non-inoculated control leaves of A17 and DZA. (B) Venn diagrams showing shared and unique up- (up arrow) and down-regulated (down arrow) genes in A17 and DZA. (C) Validation of selected *Mt* DEGs upon *Ep* inoculation. Bar plot and inset scatter plot show a comparison of RNA-Seq and qPCR $\log_2$ fold change values obtained for 15 differentially expressed genes at 1 dpi. qPCR values represent mean $\log_2$ fold change values (ddCt ± SEM) at 1 dpi compared with 1 d non-inoculated controls from three independent biological replicate experiments. *MtUBQ* served as the endogenous control for normalization. The inset scatter plot highlights the high correlation between both methods (r = 0.87). Gene IDs are provided in Supplementary Table S1.

wise read mapping statistics. As expected, we found that the vast majority of HQ reads in control samples mapped to *Mt* transcripts whereas the inoculated samples also contained a small percent of reads that mapped to *Ep* transcripts, ranging from 0.005% in A17 to 0.02% in DZA (Supplementary Table S6).

3.3. Differential transcriptional response to Ep infection in resistant and susceptible Mt

About twice as many DEGs were detected in A17 (1495) compared to DZA (751) (Fig. 2A). This difference was more evident in the up-regulated set, with nearly 2.8× more genes induced in A17 (1290) compared to DZA (452), and less pronounced in the down-regulated set with 205 genes repressed in A17 compared to 299 in DZA. Majority of the DEGs were unique to a particular interaction with few genes detected in the up-regulated (290) or down-regulated [26] sets of both genotypes (Fig. 2B). Within the shared up-regulated gene set, fold change values were higher in A17 compared to DZA (Supplementary Datasheet S1).

To validate the RNA-Seq data, we performed qPCR for 15 genes that were selected based on differential expression in A17 and DZA. As shown in Fig. 2C, the expression patterns obtained by qPCR paralleled those obtained through RNA-Seq for most genes, with a Pearson's correlation coefficient of 0.87 ($p < .0001$).

3.4. Ep-impacted host functional processes during an incompatible interaction

To delineate the transcriptional changes that occur during incompatible and compatible *Mt–Ep* interactions, we subjected A17 and DZA DEGs with Mt4.0 v2 IDs to functional enrichment analysis against the *Mt* genome as background. GO biological process terms exclusively enriched in the A17 DEG dataset mainly grouped into five categories: cell recognition, protein phosphorylation, macromolecule modification, cellular amino acid metabolism, and phenylpropanoid biosynthesis (Fig. 3A; Supplementary Datasheet S2). MapMan bins exclusively over-represented in A17 DEGs include pathways such as signaling and amino acid/protein synthesis, and protein families such as PR-proteins, glutathione-S-transferases, GCN5-related N acetyltransferases, *O*-methyl transferases, myrosinases-lectin-jacalin, peroxidases, cytochrome P450,

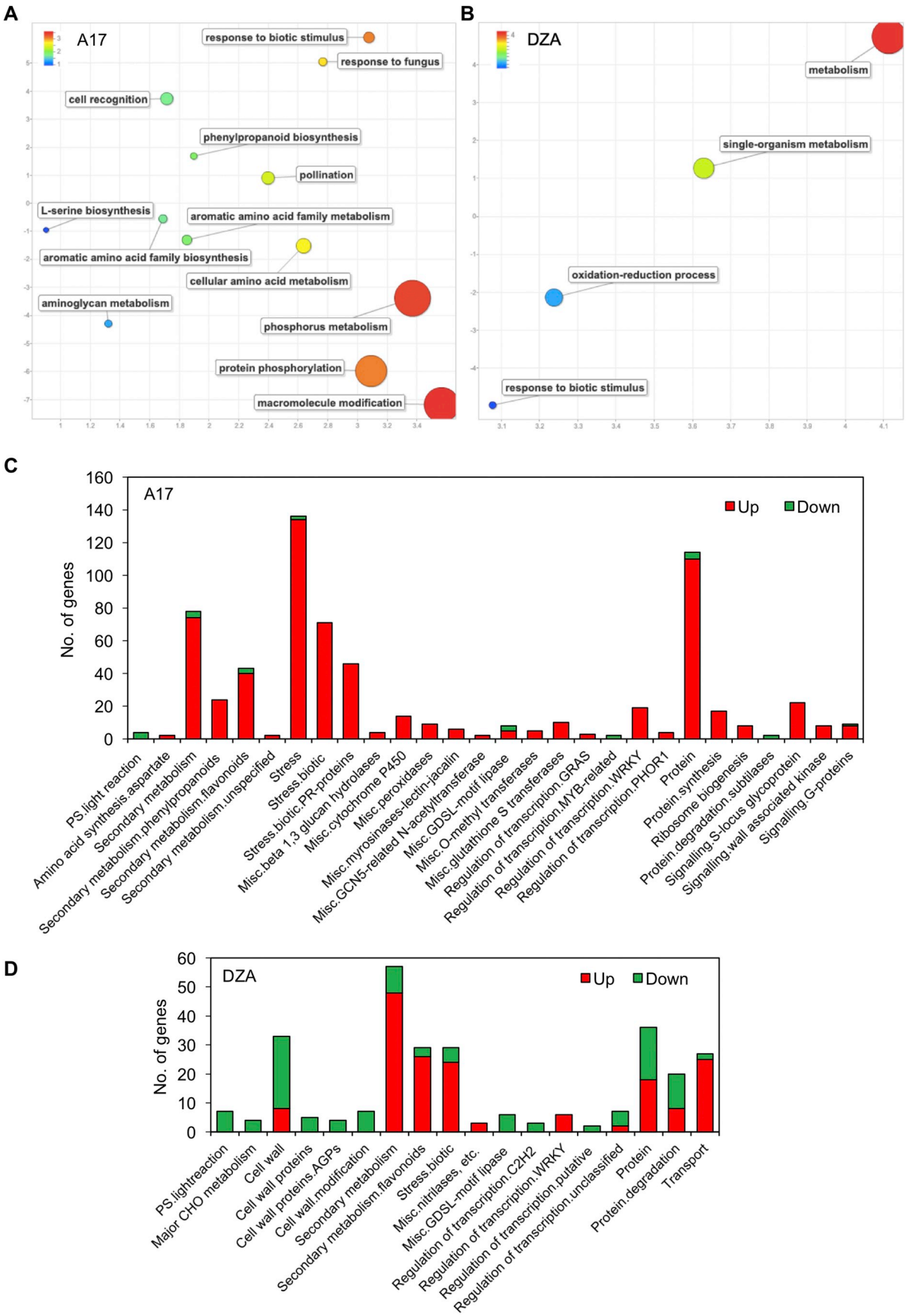

(caption on next page)

Fig. 3. Enriched gene ontology (GO) biological process terms and MapMan bins in A17 and DZA DEGs. (A-B) GO enrichment ($p \leq .05$) was performed using MedicMine (http://medicmine.jcvi.org) and enriched terms with 2 or more genes were summarized using REVIGO semantic analysis to remove redundant GO terms. Bubble colour indicates the $\log_{10}$ *p*-value (scale in the upper right-hand corner of each plot); bubble size indicates the number of genes associated with a particular GO term. (C-D) Enriched MapMan categories or sub-categories ($p \leq .05$). Red bar, up-regulated genes; green bar, down-regulated genes. (For interpretation of the references to colour in this figure legend, the reader is referred to the web version of this article.)

and ß-1,3 glucan hydrolases (Fig. 3C; Supplementary Datasheet S3). Notably, all genes classified under the GO and MapMan categories were up-regulated in A17 in response to *Ep*.

Genes classified under the cell recognition GO category and MapMan signaling bin predominantly encode members of different cell surface-localized RLK families, including *WAKs*, *leucine-rich repeat (LRR)-RLKs*, *cysteine-rich-RLKs*, *lectin-RLKs*, and *LysM type-RLKs*. Genes classified under the protein phosphorylation GO category include several defense-signaling components such as *serine/threonine protein kinases*, *mitogen-activated protein kinase* (*MAPK*) and *MAPKK*. In addition to *RLK*s, the macromolecule modification GO category contains 3 *plant U-box type E3 ubiquitin ligase* (*PUB*) genes: *PUB14*, *Avr9/Cf9 rapidly-elicited gene PUB20,* and *PUB23*. This GO category also contains 3 genes encoding subunits of the oligosaccharyl transferase STT3 complex involved in N-glycosylation. The amino acid synthesis GO category and MapMan bin include genes mainly involved in aromatic and polar amino acid synthesis. The PR-protein MapMan bin includes several *chitinases* and Toll/interleukin-1 receptor (TIR) type *NLR* genes.

3.5. Ep-impacted host functional processes during a compatible interaction

GO terms exclusively enriched in DZA DEGs include metabolism and oxidation-reduction process, and enriched MapMan bins include major carbohydrate metabolism, transport, and cell wall (Figs. 3B & D; Supplementary Datasheets S2-S3). The metabolism and oxidation-reduction process GO categories is dominated by genes encoding proteins involved in redox reactions such as peroxidases, lipoxygenase, alternative oxidase, 2OG-Fe (II) oxygenase, ACC oxidase, aldo/keto reductase, and members of the cytochrome P450 family. A number of these enzymes are either known to play a direct role in ROS/reactive aldehyde detoxification, or involved in the synthesis of secondary metabolites with antioxidant/antimicrobial properties. For example, genes encoding an alternative oxidase, known to mitigate ROS accumulation in mitochondria, superoxide dismutase, known to catalyze the dismutation of superoxide radicals to oxygen and hydrogen peroxide [68], and an NADP-dependent alkenal double bond reductase, known to detoxify reactive aldehydes [69], were significantly up-regulated in DZA. The major carbohydrate metabolism MapMan bin includes genes involved in starch synthesis and degradation, all of which were down-regulated only in DZA. The transport bin contains genes encoding phosphate transporters, a nitrate transporter, zinc transporters, sugar/H^+ symporters, ABC transporters, and MATE efflux transporters. Within the cell wall bin, genes involved in cell wall synthesis and modification such as *cellulose synthases*, *expansins*, *polygalacturonases*, *pectinesterases*, *xyloglucan endotransglucosylase/hydrolases*, and *fasciclin-like arabinogalactans* were exclusively down-regulated in DZA.

3.6. Ep-impacted host processes impacted during incompatible and compatible interactions

Few GO and MapMan categories were significantly enriched in both A17 and DZA DEG datasets. These include response to biotic stimulus, biotic stress, secondary metabolism, protein degradation, photosynthesis, and GDSL-motif lipase (Fig. 3; Supplementary Datasheets S2–S3). The response to biotic stimulus and biotic stress categories in both datasets are dominated by *PR*-genes and *NLR*s, but fewer genes and lower fold change induction values were detected in DZA compared to A17. A similar pattern was observed for the secondary metabolism MapMan bin, which includes genes involved in the isoflavonoid and lignin biosynthetic pathways. In contrast, a greater number of genes encoding different types of proteases, components of the ubiquitin pathway, chlorophyll *a*/b-binding proteins and GDSL-motif lipases were down-regulated in DZA compared to A17.

3.7. Ep- impacted transcription factors and enriched cis-acting elements in co-regulated promoters

Transcriptional regulation plays a central role in the activation or suppression of expression during pathogen infection and is largely controlled through transcription factors (TFs) and regulatory cis-elements present in gene promoters. Notably, 'Regulation of transcription' was identified as an enriched MapMan bin in both A17 and DZA DEGs (Fig. 3). To identify regulatory factors associated with incompatible and compatible *Mt-Ep* interactions, we (1) identified TFs with infection-altered expression in A17 and DZA (Table 1) and (2) analyzed the 1-kb promoters of DEGs for significantly enriched cis-acting regulatory motifs or TF-binding sites (TFBS) (Table 2; Supplementary Datasheet S4). We found 61 TFs in A17 and 25 in DZA with significantly altered expression in response to *Ep*. Of these, 9 were significantly up-regulated in both genotypes.

The WRKY family was the largest and the only statistically enriched TF family in both datasets (Fig. 3); however, differences in the number and expression of WRKY TFs were observed between A17 and DZA (Table 1). Nineteen *WRKY*s were induced in A17 whereas only 6 were induced in DZA, with fold change values lower in DZA in all cases. In line with this, the WBOX motif, bound by WRKY TFs, was more strongly enriched in A17 up-regulated gene promoters compared to DZA (Table 2). A search for *Arabidopsis* orthologs of induced *MtWRKYs* revealed that 9/21 show sequence similarities to *AtWRKYs* previously implicated in the regulation of SA biosynthesis and/or signaling (Table 1). These include AtWRKY75 [70], a positive regulator of SA biosynthesis, AtWRKY70, AtWRKY54, AtWRKY50, and AtWRKY51, positive regulators of SA signaling [71–73], and AtWRKY33 and AtWRKY40, negative regulators of SA-dependent defense responses [74,75].

The ERF family was the second largest TF family with *Ep* infection-altered expression. In general, ERFs were up-regulated in A17 but down-regulated in DZA. Three *MtERF*s up-regulated in A17 show similarities to *AtERF1* or *AtERF59*, which are positive regulators of the JA/ET signaling pathway [76,77]. In contrast, an *MtERF* (*Medtr4g100450*) similar to *AtERF5/AtERF6*, both known positive regulators of JA-mediated defense responses [78], was down-regulated in DZA. Additionally, a homolog of AtERF8, a PCD-inducer [79], was down-regulated only in DZA.

MYB TFs were significantly impacted by *Ep* predominantly in A17. Six MYBs were significantly up-regulated and 3 down-regulated only in A17. One of the up-regulated MtMYBs is similar to the soybean MYB29, which is a positive regulator of isoflavonoid biosynthesis [80]. In accordance with this, the L1DCPAL1 motif bound by MYB TFs and present in the promoter of the *phenylalanine ammonia-lyase* (*PAL*) gene [81] that encodes the first enzyme of the phenylpropanoid pathway, was strongly enriched in A17 up-regulated promoters.

C2H2, NAC, GRAS and Trihelix TF family members were either exclusively up-regulated in A17 or exclusively down-regulated in DZA. In accordance with this, C2H2-, NAC-, and Trihelix TF-binding motifs were strongly enriched only in A17 up-regulated promoters. Two *C2H2* TFs up-regulated in A17 are similar to *AtZAT6*, which plays an important role in H_2O_2-activated anthocyanin synthesis [82]. A *C2H2*

Table 1
Transcription factors with altered expression at 1 dpi of *Ep* infection in A17 and/or DZA.

Transcription Factors		*Arabidopsis thaliana* ortholog[3]		Log_2 fold change[4]	
Mt ID[1]	TF Family[2]	ID	Gene Name	A17	DZA
Medtr8g044070	AP2	*AT3G54320*	*WRI1*	**2.9**	**2.0**
Medtr7g092540	bHLH			**1.4**	0.5
Medtr2g039620	bHLH	*AT5G56960*	*bHLH*	**7.9**	**2.5**
Medtr5g017210	bHLH	*AT5G67060; AT3G50330*	*HEC1; HEC2*	**-3.5**	-1.5
Medtr1g096530	bHLH	*At2g47270*	*UPBEAT1*	**-4.7**	-0.7
Medtr4g070320	bHLH	*AT4G34530*	*CIB1*	**-1.2**	-0.8
Medtr8g067280	bHLH	*AT1G32640*	*MYC2*	1.0	**-2.7**
Medtr1g022495	bZIP	*AT4G34590*	*bZIP11*	-0.4	**1.8**
Medtr4g079500	bZIP	*AT2G42380; AT3G58120*	*bZIP34; bZIP61*	0.8	**-1.8**
Medtr3g102980	C2H2	*AT1G27730; AT5G04340*	*STZ; ZAT6*	**1.3**	-0.4
Medtr1g018420	C2H2	*AT1G27730; AT5G04340*	*STZ; ZAT6*	**2.6**	0.0
Medtr1g093095	C2H2	*AT1G13290*	*DOT5*	-0.9	**-4.1**
Medtr7g100100	C2H2	*AT2G37430; AT3G53600*	*ZAT11; ZAT18*	0.9	**-1.9**
Medtr1g106730	C2H2			0.7	**-1.0**
Medtr5g071070	C3H	*AT2G40140; AT3G55980*	*CZF1; SZF1*	**2.2**	0.3
Medtr4g078660	C3H			**-1.7**	-1.7
Medtr8g090205	CAMTA	*AT2G22300*	*SR1*	**1.5**	0.0
Medtr2g013370	Dof			**-2.0**	-1.8
Medtr4g109980	Dof	*AT5G60850*	*OBP4*	-0.6	**-1.0**
Medtr7g096830	ERF	*AT1G06160; AT2G31230*	*ERF59; ERF15*	**1.4**	**1.0**
Medtr5g075570	ERF			**1.5**	0.3
Medtr1g069945	ERF	*AT1G06160; AT2G31230*	*ERF59; ERF15*	**1.5**	-0.1
Medtr2g014300	ERF	*AT1G28360*	*ERF12*	**2.1**	0.0
Medtr1g043350	ERF	*AT3G23240*	*ERF1*	**2.3**	0.8
Medtr2g015040	ERF			**2.3**	-0.1
Medtr1g074370	ERF			**2.9**	-0.3
Medtr7g020980	ERF			**-1.3**	0.8
Medtr6g037610	ERF	*AT5G64750*	*ABR1*	-	**3.4**
Medtr5g062700	ERF			-0.8	**-1.6**
Medtr4g100450	ERF	*AT4G17490; AT5G47230*	*ERF6; ERF5*	-0.3	**-1.3**
Medtr2g078680	ERF	*AT1G53170; AT3G15210*	*ERF8; ERF4*	0.4	**-1.1**
Medtr2g038720	GATA	*AT4G26150; AT5G56860*	*CGA1*	**-3.0**	0.4
Medtr2g097463	GRAS			**1.0**	-0.6
Medtr4g133660	GRAS	*AT4G17230*	*SCL13*	**1.1**	-0.8
Medtr5g094450	GRAS			**1.1**	1.0
Medtr4g064160	GRAS	*AT1G07530; AT2G29060*	*SCL14*	-1.1	**-1.7**
Medtr8g469430	HD-ZIP			**1.9**	0.9
Medtr5g019650	HD-ZIP	*AT2G18550; AT4G36740*	*HB21; HB40*	**-2.0**	-1.2
Medtr1g101280	HD-ZIP			0.2	**-1.5**
Medtr8g105780	HSF	*AT1G67970*	*HSFA-8*	**1.3**	0.4
Medtr5g017470	HSF	*AT4G36990*	*HSF4*	**3.3**	**1.4**
Medtr7g110830	MYB			**1.3**	0.8

(*continued on next page*)

Table 1 (*continued*)

Medtr1g043050	MYB	*AT1G06180; AT2G31180*	*MYB13; MYB14*	**1.5**	0.1
Medtr1g076150	MYB	*AT1G06180; AT2G31180*	*MYB13; MYB14*	**1.6**	0.4
Medtr1g043080	MYB	*AT1G06180; AT2G31180*	*MYB13; MYB14*	**2.0**	0.2
Medtr3g101290	MYB			**3.3**	0.0
Medtr8g027345	MYB			**7.5**	**2.7**
Medtr7g011170	MYB	*AT3G01140; AT5G15310*	*MYB106; MYB16*	**-3.5**	-0.9
Medtr4g046737	MYB			**4.4**	1.8
Medtr6g004250	MYB			**-3.2**	-0.8
Medtr6g092540	MYB	*AT5G56840*		**-1.7**	-0.1
Medtr4g075980	NAC	*AT2G17040*	*ANAC036*	**1.4**	0.0
Medtr2g079990	NAC	*AT1G52890; AT3G15500*	*ANAC019; NAC3*	**1.6**	0.6
Medtr5g090970	NAC	*AT2G43000*	*ANAC042*	**2.4**	2.7
Medtr4g052620	NAC	*AT3G44350; AT5G22380*	*ANA061; NAC090*	-	**-3.2**
Medtr8g059170	NAC	*AT4G27410*	*RD26*	0.7	**-1.0**
Medtr4g088555	SBP	*AT2G33810*	*SPL13*	**1.5**	-0.1
Medtr2g098080	Trihelix			**4.7**	-1.7
Medtr7g073380	WRKY	*AT1G66550; AT1G66560*	*WRKY67; WRKY64*	**1.2**	-0.3
Medtr5g074400	WRKY	*AT2G38470*	*WRKY33*	**1.5**	0.1
Medtr8g027860	WRKY			**1.9**	0.3
Medtr4g082580	WRKY			**2.1**	0.0
Medtr3g031220	WRKY	*AT2G38470*	*WRKY33*	**2.3**	0.8
Medtr7g073430	WRKY	*AT1G66550; AT1G66560*	*WRKY67; WRKY64*	**2.7**	0.0
Medtr7g117200	WRKY			**2.7**	0.0
Medtr3g095040	WRKY	*AT5G64810*	*WRKY51*	**2.8**	-0.1
Medtr3g106060	WRKY			**2.9**	0.9
Medtr3g093830	WRKY	*AT2G40750; AT3G56400*	*WRKY54; WRKY70*	**3.2**	0.3
Medtr1g015140	WRKY	*AT5G26170*	*WRKY50*	**3.4**	0.8
Medtr3g104750	WRKY	*AT5G26170*	*WRKY50*	**3.5**	0.8
Medtr7g028710	WRKY	*AT5G13080*	*WRKY75*	**3.8**	**1.5**
Medtr2g105060	WRKY	*AT1G80840*	*WRKY40*	**4.1**	0.3
Medtr8g092010	WRKY	*AT5G64810*	*WRKY51*	**6.1**	**1.5**
Medtr3g090860	WRKY			**6.4**	0.3
Medtr1g013760	WRKY			**6.5**	0.8
Medtr2g045360	WRKY			**6.7**	**2.1**
Medtr1g013790	WRKY			**8.0**	**2.1**
Medtr6g038890	WRKY			0.6	**2.0**
Medtr4g107970	WRKY	*AT5G15130*	*WRKY72*	-	**2.1**

[a]*Mt* ID as per Mt4.0v2 annotation (http://www.medicagogenome.org/downloads).
[b]Transcription factor family (TF) based on Plant Transcription Factor Database v3.0 (http://planttfdb.cbi.pku.edu.cn/).
[c]*Arabidopsis thaliana* ortholog identified through MedicMine (http://medicmine.jcvi.org/medicmine/begin.do). Ortholog description from TAIR10 (https://www.arabidopsis.org/index.jsp).
[d]Values in bold represent significant changes in expression ($p \leq .05$). Red, ≥2-fold up-regulated; green, ≥2-fold down-regulated; yellow, unaltered, −, not detected.

down-regulated only in DZA is similar to *AtZAT11*, which was previously shown to be involved in oxidative stress-induced PCD [83]. Within the NAC family, one of the *NACs* up-regulated only in A17 is similar to *AtANAC019*, an activator of JA-induced defense responses [84]. A *NAC* down-regulated only in DZA is similar to *AtANAC090*, which acts in concert with *AtANAC017* and *AtANAC082* to suppress leaf senescence-promoting processes [85].

A number of bHLH TFs were significantly down-regulated only in A17. These *MtbHLHs* show similarities to the *Arabidopsis* genes *UPBEAT1, HECTATE1*, or *CIB1*, all of which are known to regulate different developmental processes in *Arabidopsis* [86], [87], [88]. Further, a homolog of *AtMYC2*, the master regulator of the JA signaling pathway [89], was significantly down-regulated only in DZA. Consistent with this, the MYCCONSENSUSAT motif was enriched in promoters of DZA down-regulated promoters.

The promoter analysis also identified the GGNCCC motif, bound by TCP TFs, as one of the most strongly enriched cis-elements in promoters of A17 and DZA (Table 2). Interestingly, a greater number of up-regulated gene promoters contain this motif in A17 whereas only down-regulated promoters harbor this motif in DZA. Surprisingly, no TCP TFs known to bind this element were identified as differentially expressed in response to *Ep*.

3.8. Functional annotation of Ep genes and identification of effector candidates

To validate the identified 140 *Ep* genes, we amplified a subset of 17 candidate genes from *Ep* conidial genomic DNA. All 17 genes amplified from *Ep* genomic DNA but not from DZA genomic DNA (Supplementary Fig. S4), confirming that they are bona fide fungal genes. Blast2GO analysis revealed that GO biological process terms such as translation, RNA-dependent DNA biosynthetic process, and nucleic acid phosphodiester bond hydrolysis were the most abundant, followed by DNA metabolic process, transcription and respiration (Fig. 4A). A search for functional Pfam protein domains identified ribosomal protein as the most abundant functional domain.

Candidate *Ep* effectors (*Ep*EFs) were predicted from proteins having a genuine start codon based on criteria used to define effectors in other PM species [90]. Based on these criteria, 5 sequences (*Ep*EF01–05) ranging in length from 32 to 66 amino acids were identified as effector candidates (Supplementary Table S7). To increase the effector repertoire, we also included 2 sequences (*Ep*EF06–07) that show similarities to previously predicted effectors from other sequenced PMs. *Ep*EF sequences were also scanned for the presence of the Y/F/WxC motif, the only motif reported to be conserved in PM effectors thus far [90]. Only *Ep*EF01 contained a YHC motif, with the motif located within 30 amino acids of the signal peptide.

We used qPCR to study the expression profiles of *EpEF* genes over the course of infection on the susceptible host DZA (Fig. 4B). *EpEF01* showed a steady increase in expression from 12 to 48 hpi, after which its expression remained high. *EpEF02* showed increased expression at 12 and 120 hpi, corresponding to penetration and asexual reproduction stages. *EpEF03* was induced only during penetration (12 hpi) and remained unchanged or suppressed at all other time points. *EpEF05–6* exhibited increased expression between 6 and 24 hpi, corresponding to the appressorium formation, penetration and primary haustorium formation stages. Unexpectedly, *EpEF07* showed reduced expression at all infection time points compared to 0 hpi.

4. Discussion

This study describes the dual RNA-Seq-based transcriptome profiling of *Mt* and the pea PM *Ep* at an early infection time point (1 dpi) during compatible and incompatible interactions. Analysis of *Ep* infection-responsive *Mt* DEGs revealed a greater degree of transcriptional reprogramming in A17 compared to DZA. This is consistent with an R protein-triggered ETI response, which is generally correlated with massive alterations of the host transcriptome [91]. We validated our findings by performing qPCR analysis on a subset of *Mt* genes. Overall, differential expression values obtained by RNA-Seq and qPCR were comparable; only 3 genes deviated from the norm: iso*flavone synthase*, *wall-associated kinase (WAK)*, and *SAUR-like auxin responsive protein*. We speculate that this may be due to the inherent high biological variability (changes in gene expression that are variable between controlled measurements) of these particular genes.

To investigate the nature of PM-induced transcriptional changes associated with resistance/susceptibility, we compared functional terms enriched in A17 and DZA DEGs. Similar to previous microarray studies that profiled *Mt-Ep* interactions at earlier time points [4 and 12 hpi; [30,32]], we found that genes encoding PR-proteins and phenylpropanoid [(iso)flavonoids and lignin] pathway enzymes were induced to a greater extent in A17 compared to DZA. Further, as reported previously, our data supports the involvement of the phytohormone SA in both *R*-gene and basal resistance against *Ep* in *Mt*. However, by adopting a dual RNA-Seq approach and a different infection time point (1 dpi), we uncovered (1) additional infection-responsive transcriptional changes during compatible and incompatible interactions, and (2) *Ep* candidate effectors that were not identified previously. We mainly focus our discussion on these novel findings in the following sections.

4.1. R-gene mediated PM resistance correlates with a strong amplification of PTI signaling

Strikingly, in contrast to previous studies, we found an over-representation of ETI-inducing *NLR* and PTI-inducing *RLK* genes exclusively in the A17 up-regulated data set. Studies on resistance signaling in plants have shown that some NLRs function as sensors of pathogen effectors or effector activities and initiate immune responses, while others act as signaling components, contributing to defense relay and amplification [92]. Therefore, it is possible that an NLR, like MtREP1, serves as the primary sensor that recognizes the pathogen signal and initiates ETI, while induction of other *NLRs* is required to amplify the resistance response in A17. In addition to *NLRs*, a number of *WAK*, *LysM-* and *lectin-type RLKs* known to activate PTI against fungal pathogens via recognition of chitin [20] or cell wall fragments [93] were induced only in A17. This suggests that PTI or basal defense is also activated to a greater extent during incompatible interactions. Pathogen signals perceived by RLKs and NLRs generally trigger similar sets of immune responses, such as ROS accumulation, Ca^{2+} spikes, MAPK cascades, transcriptional reprogramming and production of phytohormones, suggesting that PTI and ETI share the same core machinery to trigger defense [92]. Even though they share a similar framework, immune signaling responses in ETI are normally amplified and of a longer duration than they are in PTI. Collectively, our data suggests that a similar resistance mechanism might operate in A17, where an R-protein like MtREP1 triggers an ETI-mediated amplification of PTI signaling. In support of this, in addition to the PAMP/DAMP-perceiving *RLKs*, a number of genes encoding early PTI signaling components were significantly up-regulated only in A17.

4.2. The JA/ET signaling network may contribute positively to ETI against PM

The SA and jasmonic acid (JA)/ethylene (ET) signaling sectors are generally antagonistic and important for immunity against biotrophic and necrotrophic pathogens, respectively [94]. We found that the expression pattern in DZA generally supports this hypothesis; TFs with similarities to *AtWRKY51* and *AtWRKY75*, which function as positive regulators of the SA signaling network, were up-regulated, while a homolog of *AtMYC2*, an activator of JA response genes, was down-regulated. By contrast, in addition to positive regulators of the SA signaling pathway, a number of WRKY, ERF and NAC TFs with similarities

Table 2
Over-represented cis-acting elements or transcription factor-binding sites (TFBS) in promoters of DEGs and interacting TF families. 1 kb upstream promoters of DEGs were analyzed using the 'Regulation Prediction' tool in PlantRegMap v4.0 [53] with *p*-value cutoff ≤0.05. TFBS were grouped based on their interacting TF family. Motifs present in > 10 target promoters for at least one data set are shown here. Full analysis is presented in **Supplementary Datasheet S4**. TFBS motif names were obtained from PLACE [54].

TFBS	PLACE motif name	TF known to bind TFBS	No. of DEGs with TFBS			
			A17 up	A17 down	DZA up	DZA down
	WBOX	WRKY	130	-	21	-
	PALINDROMICCBOXGM	bZIP	31	-	6	-
	-	TCP	129	12	-	44
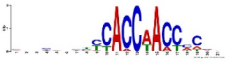	L1DCPAL1	MYB	135	-	63	-
	-	MYB	165	9	74	20
	-	MYB	-	10	19	-
	MBSI	MYB	-	3	7	17
	MYBST1	MYB	-	13	-	-
	-	NAC	112	7	-	-
	-	C2H2	70	-	-	30
	ATHBATCONSENSUS	HD-ZIP	25	6	-	-
	DE1PSPRA2	Trihelix	47	-	-	-
	-	CPP	36		15	9
	MYCCONSENSUSAT	bHLH	-	-	-	18
	-	bHLH	-	-	-	13
	CURECORECR	SBP	-	8	14	4
	HSE	HSF	-	-	12	-
	HD WUS-like	WOX	-	-	-	16

to *Arabidopsis* TFs that function as positive regulators of the JA/ET signaling network, such as *WRKY33* [74], *WRKY40* [75], *ERF1* [76], *ERF59* [77], and *ANAC019* [84], were significantly up-regulated only in A17. This suggests that JA-mediated responses may also contribute to immunity during incompatible interactions. Interestingly, several studies have reported that SA and JA accumulate to high levels particularly during ETI [e.g. [95,96]]. This coordinated up-regulation of SA and JA/ET signaling networks might provide a mechanism by which plants can use PCD as a major defense mechanism against biotrophic pathogens without making them vulnerable to necrotrophic pathogens [95]. Alternatively, the JA/ET signaling network may contribute positively to immunity by compensating for any pathogen-triggered loss/perturbation in the SA signaling network [97].

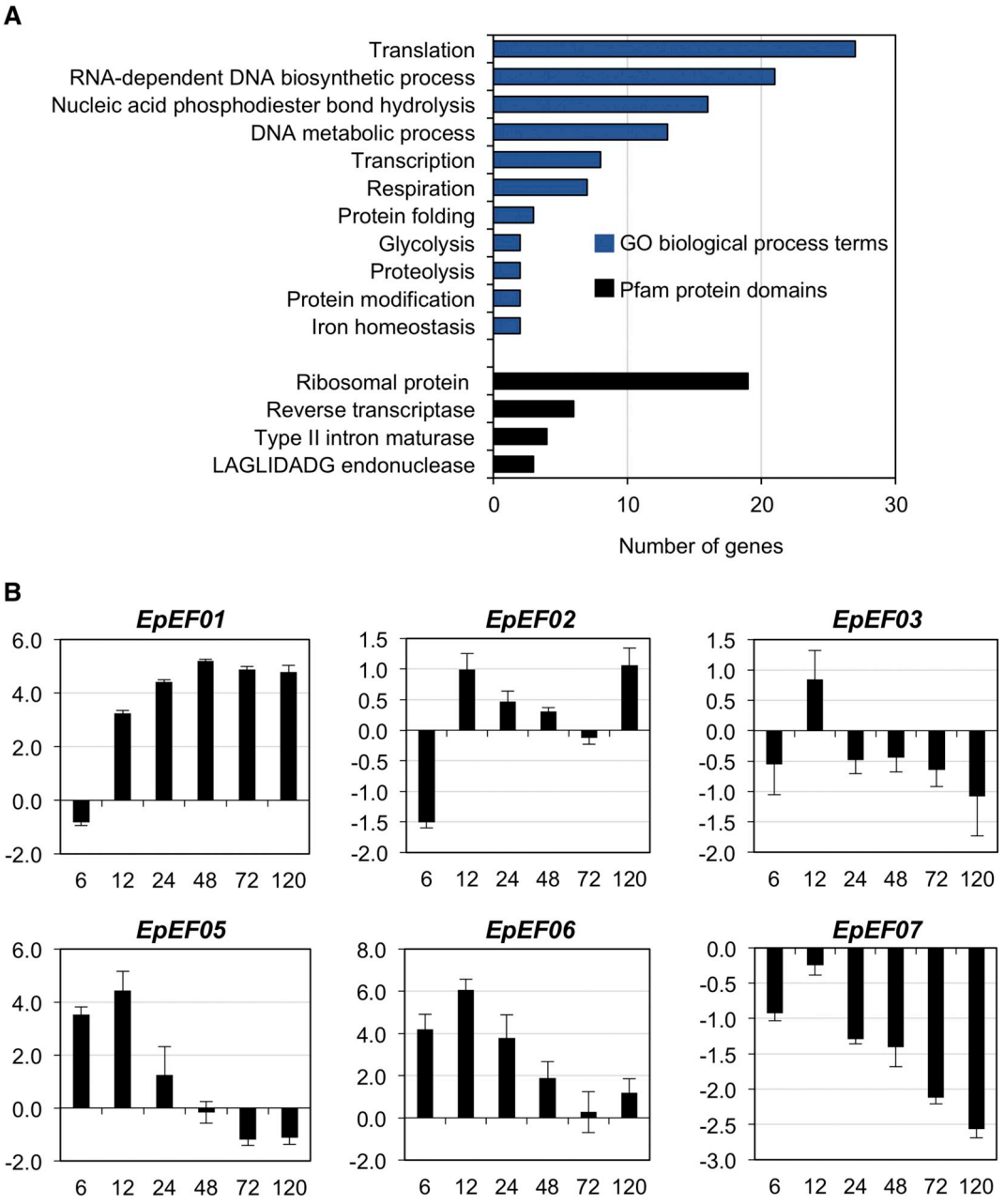

Fig. 4. Functional enrichment of *Ep* genes and temporal expression analysis of *EpEF*s. (A) Top GO terms and protein domains associated with *Ep* genes. GO biological process and Pfam domain categories containing ≥2 genes are shown here. (B) *In-planta* temporal expression profiles of *EpEF*s determined by qPCR analyses of *Ep*-inoculated DZA leaf samples. *x* axes represent hours' post inoculation (hpi). *y* axes represent the mean $\log_2$ fold change values (ddCt ± SEM) at different time points of infection (6–120 hpi) compared with 0 hpi from three independent biological replicate experiments. *EpTub2* served as the endogenous control for normalization.

4.3. Regulation of growth-defense balance may lead to effective PM resistance

Defense activation against pathogens often occurs at the expense of plant growth. Consequently, plants use different strategies to mitigate this growth-defense tradeoff, such as, temporarily diverting resources from growth towards defense, controlling the timing and duration in which the immune response is active, and defense priming [98,99]. As discussed below, our expression data suggests that some of these mechanisms may operate more strongly in A17. In addition to the transcriptional repression of photosynthesis-related genes, an energy-conserving response generally observed in response to PM infection [100], down-regulation of development-related regulators such as *HD-ZIP* and *bHLHs* was observed in A17. Also, homologs of TFs known to regulate growth-defense transitions in *Arabidopsis*, such as *HSF4* [101] and *Trihelix* [102], were significantly up-regulated only in A17. This suggests that during incompatible interactions, resources are efficiently diverted from growth towards immunity. In support of this, our analysis of co-regulated promoters identified TCP TF-binding motifs as strongly enriched in A17 DEG promoters. TCPs are plant-specific TFs, which act at the interface of plant growth and defense by regulating a myriad of cellular processes ranging from cell proliferation to immunity [103,104]. Members of this family positively regulate defense by targeting promoters of defense-related genes, including *PR* and *NLR* genes [105,106]. Interestingly, we found that A17 up-regulated genes carrying TCP-binding elements in their promoters are mainly associated with defense-related processes (Supplementary Table S8).

Continuous activation of defense by PAMPs and DAMPs can also

have deleterious effects on plant growth; therefore, tight control over these signaling events is required to limit spurious activation of defense. Studies in *Arabidopsis* have revealed that ubiquitination and N-glycosylation play important roles in regulating immune responses by influencing RLK abundance and pathogen recognition. For example, the *Arabidopsis* E3-ubiquitin ligase PUB23 acts in concert with two other PUBs to dampen PTI signaling by targeting PRRs for degradation via ubiquitination [107,108]. Another study showed that the *Arabidopsis* EFR receptor kinase lacking a single conserved N-glycosylation site accumulated to lower levels and lost the ability to bind to its ligand (bacterial translational elongation factor Tu/elf-18) and mediate ligand-induced oxidative burst [109]. We found that homologs of *Arabidopsis PUB*s and *STT3* subunits were up-regulated only in A17, suggesting that post-translational regulation of PRR stability and function may help regulate the timing and duration of defense signaling [110].

4.4. Suppression of defense signaling, PCD, and cell wall synthesis/modification correlates with PM susceptibility

One way by which *Ep* can promote biotrophy is through a general suppression of pathogen perception and host defense signaling. A recent review on pathogen effectors revealed that, in terms of molecular function, NLRs, ubiquitination and kinases make up almost 60% of fungal effector targets [21]. The fact that fewer *Mt* genes with these molecular functions were up-regulated in DZA suggests that these genes may be targets of *Ep* effectors. Moreover, enhanced detoxification of ROS and reactive aldehyde species may be critical to prevent or limit ROS-induced oxidative damage and PCD in response to the biotrophic PM pathogen. In line with this, genes encoding enzymes involved in ROS/reactive aldehyde detoxification were significantly up-regulated in DZA, whereas homologs of positive regulators of PCD, such as *AtERF8* and *AtZAT11*, were down-regulated. Further, the down-regulation of genes encoding proteases and ubiquitin-mediated protein degradation pathway components, which function in PCD [111], supports the idea that PCD suppression is integral to *Ep* susceptibility.

Strengthening of plant cell walls at the sites of attempted fungal attack through the development of cell wall appositions, called papillae, is an important aspect of penetration resistance against PMs. A study on barley-*Bgh* interactions showed that higher concentrations of callose, cellulose, and arabinoxylan are present in effective papillae compared to ineffective papillae [112]. Additional studies have suggested that AGPs may help strengthen this cell wall barrier by crosslinking with arabinoxylan [113,114]. Notably, cellulose synthase and AGP-encoding genes were down-regulated only in DZA, correlating with the weaker penetration resistance observed during compatible interactions.

4.5. Ep effector candidates and genes as putative pathogenicity factors

Although deep sequencing was performed, the percentage of pathogen reads detected in the infected samples was at the lower end of the range (~0.02–0.1%) previously reported in other plant-pathogen dual RNA-Seq studies conducted at similar infection time points [115]. We reasoned that this may be a consequence of low fungus-to-plant biomass ratio at 1 dpi and/or unavailability of a complete reference genome for *Ep*. Nevertheless, 140 *Ep* transcripts were identified from which 7 *Ep*EF candidates were predicted. Interestingly, ~66% of these transcripts were also detected in *Ep* haustoria enriched from 6 dpi pea leaves (Supplementary Table S5; [29]). However, the effector candidates identified in this study were not detected in the haustorial sample. This implies that *Ep* expresses specific sets of effectors at distinct infection stages and on different hosts (pea versus *Mt*). Indeed, temporal expression analysis revealed that *EpEFs* exhibit infection stage-specific expression patterns. *EpEF03*, *EpEF05* (similar to *Bgh* CSEP0051 [116]), and *EpEF06* are expressed early during infection and may therefore contribute to virulence during the initial stages of colony establishment. *Ep*EF06 encodes an *Egh16H1-like* gene that belongs to one of the largest gene families characterized in *Bgh* with homologs present in all pathogenic fungi [117]. *Bgh Egh16H* and its homologs *GAS1* and *GAS2* in the rice blast fungus *Magnaporthe grisea* [118] and *Magas1* in the entomopathogenic fungus *Metarhizium acridum* [119] were previously reported to be expressed mainly during appressorium formation, penetration and/or haustorium formation. Mutants deleted in *GAS1*, *GAS2*, or *Magas1* were defective in penetration and showed reduced virulence on their respective hosts indicating that *Egh16H* homologs are important virulence factors required for pathogenesis. Interestingly, an *Egh16H*-like gene was also identified in the *Ep* haustorial transcriptome but was predicted to be a secreted non-effector protein [29]. Host induced gene silencing of this gene in leaves of susceptible pea plants via infiltration of specific double stranded (ds)-RNAs resulted in reduced pathogen virulence, demonstrating the role of this class of genes in PM pathogenesis [29].

Sequence wise, *Ep*EF07 is most similar to the *G. orontii* effector OEC70. In a previous in vitro effector-interactome study, OEC70 was shown to interact with 6 *Arabidopsis* proteins, including a Trihelix TF, an ERF, a COP9 signalosome subunit, a ubiquitin-like protein and two TCP TFs [120]. When the functional relevance of these OEC70-interacting host proteins was tested using mutant plants, 3 out of 6 showed altered PM disease phenotypes either at seedling or adult stages, providing genetic support for their involvement in plant-PM interactions. This included a member of the TCP TF family, cis-acting elements for which were over-represented in promoters of DEGs of both A17 and DZA. It is possible that *Ep*EF07 may similarly interact with *Mt*TCP TF(s), and this interaction may impact defense gene expression during *Ep-Mt* interactions. Surprisingly, *EpEF07* expression was repressed in DZA, suggesting that *Ep* may suppress the expression of specific effectors to evade recognition by the host.

Subcellular localization of effector proteins in plant cells can provide substantial clues on the molecular and cellular basis of their virulence activities. Localization prediction tools indicated that *Ep*EF01 and *Ep*EF06 are localized to the plant apoplast. Apoplastic effectors often tend to be cysteine-rich; the disulfide bridges formed between the cysteine pairs are known to enhance the stability of these proteins in the plant apoplast, an environment rich in degradative proteases [121]. Notably, the *Ep*EF01 protein sequence is rich in cysteines, consistent with its prediction as an apoplastic effector.

In addition to effector candidates, we also identified a few non-effector *Ep* genes that may serve as pathogenicity factors. These include two genes encoding extracellular aspartyl proteases and three genes encoding heat shock proteins (HSPs): *HSP60*, *HSP70* and *HSP90*. Proteases secreted by pathogenic fungi are known to contribute to pathogenesis either by modifying/degrading components of the host defense machinery or by altering effector function via proteolytic cleavage [122–124]. Likewise, fungal HSPs are also known to contribute to virulence. For example, HSP90 was recently shown to play a crucial role in the virulence of the plant pathogenic fungus *Fusarium graminearum* [125].

5. Conclusions

In summary, our findings provide novel insights into potential resistance and susceptibility mechanisms employed by *Mt* against the pea PM pathogen *Ep* during an early infection event, and provides an initial resource for the development of PM resistance in legumes of agronomic import. The *in-planta* expressed fungal effector candidates represent a valuable resource that can be leveraged to identify *Ep*-specific pathogenicity factors and significantly improve our current understanding of the disease.

Supplementary data to this article can be found online at https://doi.org/10.1016/j.ygeno.2019.12.007.

Author contributions

DC designed the research. MG, GS, VG, AG and RG conducted the experiments. DC, MV, RB, GS and DS analyzed the RNA-Seq data. DC wrote the article with minor contributions from RB, MV, and DS.

Declaration of Competing Interests

The authors declare that they have no competing interests.

Availability of data and material

Raw sequencing data generated in this study is available at Sequence Read Archive under the accession numbers: SRR7589436, SRR7589435, SRR7589438, SRR7589437. The transcriptome Shotgun Assembly project has been deposited at DDBJ/EMBL/GenBank under the accession GHBM00000000. The version described in this paper is the first version, GHBM01000000.

Funding

This work was supported by an Innovative Young Biotechnologist Award (BT/09/IYBA/2015/12) from DBT, India, Early Career Research Award (ECR/2016/001043) from SERB, India and intramural funds from RCB, India to DC. MG was supported by a UGC-NET Research Fellowship, India and GS by a SERB-National Postdoctoral Fellowship, India (PDF/2016/000952).

Acknowledgements

We thank Dr. DK Banyal for the *Ep* isolate, Dr. Deborah Samac for *Mt* seeds and Dr. Ralph Panstruga for *G. orontii* haustorial transcriptome contig sequences.

References

[1] D.A. Glawe, The powdery mildews: a review of the world's most familiar (yet poorly known) plant pathogens, Annu. Rev. Phytopathol. 46 (1) (2008) 27–51. Available from: https://doi.org/10.1146/annurev.phyto.46.081407.104740.

[2] S. Fondevilla, D. Rubiales, Powdery mildew control in pea. A review, Agron. Sustain. Dev. 32 (2) (2012) 401–409.

[3] A. Singh, B. Bhatt, K. Singh, A. Kumar, U. Manibhushan Kumar, et al., Dynamics of powdery mildew (*Erysiphe trifolii*) disease of lentil influenced by sulphur and zinc nutrition, Plant Pathol. J. 12 (2) (2013) 71–77.

[4] D.L. Yadav, P. Jaisani, R.N. Pandey, Identification of sources of resistance in mungbean genotypes and influence of fungicidal application to powdery mildew epidemics, Int. J. Curr. Microbiol. App. Sci. 3 (2) (2014) 513–519.

[5] P.H. Smith, E.M. Foster, L.A. Boyd, J.K.M. Brown, The early development of *Erysiphe pisi* on *Pisum sativum* L, Plant Pathol. 45 (2) (1996) 302–309.

[6] R. Hückelhoven, Powdery mildew susceptibility and biotrophic infection strategies, FEMS Microbiol. Lett. 245 (1) (2005) 9–17.

[7] C.J. Ridout, Multiple Avirulence paralogues in cereal powdery mildew fungi may contribute to parasite fitness and defeat of plant resistance, Plant Cell Online. 18 (9) (2006) 2402–2414. Available from: https://doi.org/10.1105/tpc.106.043307.

[8] S. Xiao, O. Calis, E. Patrick, G. Zhang, P. Charoenwattana, P. Muskett, et al., The atypical resistance gene, RPW8, recruits components of basal defence for powdery mildew resistance in *Arabidopsis*, Plant J. 42 (1) (2005) 95–110.

[9] D. Ellinger, M. Naumann, C. Falter, C. Zwikowics, T. Jamrow, C. Manisseri, et al., Elevated early callose deposition results in complete penetration resistance to powdery mildew in Arabidopsis, Plant Physiol 161 (3) (2013) 1433–1444. Available from doi/10.1104/pp.112.211011.

[10] C. Kwon, C. Neu, S. Pajonk, H.S. Yun, U. Lipka, M. Humphry, et al., Co-option of a default secretory pathway for plant immune responses, Nature. 451 (7180) (2008) 835–840.

[11] M. Humphry, C. Consonni, R. Panstruga, *mlo*-based powdery mildew immunity: silver bullet or simply non-host resistance? Mol. Plant Pathol. 7 (6) (2006) 605–610.

[12] I. Serrano, Y. Gu, D. Qi, U. Dubiella, R.W. Innes, The *Arabidopsis* EDR1 protein kinase negatively regulates the ATL1 E3 ubiquitin ligase to suppress cell death, Plant Cell Online. 26 (11) (2014) 4532–4546. Available from: https://doi.org/10.1105/tpc.114.131540.

[13] D. Chandran, J. Rickert, C. Cherk, B.R. Dotson, M.C. Wildermuth, Host cell ploidy underlying the fungal feeding site is a determinant of powdery mildew growth and reproduction, Mol. Plant-Microbe Interact. 26 (5) (2013) 537–545. Available from: https://doi.org/10.1094/MPMI-10-12-0254-R.

[14] S. Fondevilla, C. Chattopadhyay, N. Khare, *Erysiphe trifolii* is able to overcome *er1* and *Er3*, but not *er2*, resistance genes in pea, Eur. J. Plant Pathol. 3 (2013) 557–563.

[15] S.B. Cannon, G.D. May, S.A. Jackson, Three sequenced legume genomes and many crop species: rich opportunities for translational genomics, Plant Physiol 151 (3) (2009) 970–977. Available from https://doi.org/10.1104/pp.109.144659.

[16] H. Tang, V. Krishnakumar, S. Bidwell, B. Rosen, A. Chan, S. Zhou, et al., An improved genome release (version Mt4.0) for the model legume *Medicago truncatula*, BMC Genomics 15 (1) (2014) 1–14.

[17] C. Ameline-Torregrosa, M. Cazaux, D. Danesh, F. Chardon, S.B. Cannon, M.T. Esquerre-Tugaye, et al., Genetic dissection of resistance to anthracnose and powdery mildew in *Medicago truncatula*, Mol. Plant Microbe Interact 21 (1) (2008) 61–69. Available from https://doi.org/10.1094/MPMI-21-1-0061.

[18] S. Yang, F. Tang, E.T. Caixeta, H. Zhu, Epigenetic regulation of a powdery mildew resistance gene in *Medicago truncatula*, Mol. Plant 6 (6) (2013) 2000–2003.

[19] K.E. Goff, K.M. Ramonell, The role and regulation of receptor-like kinases in plant defense, Gene Regul. Syst. Biol. 1 (2007), https://doi.org/10.1177/117762500700100015 117762500700100. Available from:.

[20] D. Tang, G. Wang, J.-M. Zhou, Receptor kinases in plant-pathogen interactions: more than pattern recognition, Plant Cell 29 (4) (2017) 618–637. Available from: https://doi.org/10.1105/tpc.16.00891.

[21] M. Khan, D. Seto, R. Subramaniam, D. Desveaux, Oh, the places they'll go! A survey of phytopathogen effectors and their host targets, Plant J. 93 (4) (2018) 651–663.

[22] J.D.G. Jones, J.L. Dangl, The plant immune system, Nature. 444 (7117) (2006) 323–329.

[23] H.R.A.L.V. Der, S. Kamoun, From guard to decoy: a new model for perception of plant pathogen effectors, Plant Cell 20 (2008) 2009–2017.

[24] P.D. Spanu, J.C. Abbott, J. Amselem, T.A. Burgis, D.M. Soanes, K. Stüber, et al., Genome expansion and gene loss in powdery mildew fungi reveal tradeoffs in extreme parasitism, Science 330 (2010) 1543–1546. Available from http://www.ncbi.nlm.nih.gov/pubmed/21148392.

[25] D. Godfrey, Z. Zhang, G. Saalbach, H. Thordal-Christensen, A proteomics study of barley powdery mildew haustoria, Proteomics. 9 (12) (2009) 3222–3232.

[26] R. Weßling, S.M. Schmidt, C.O. Micali, F. Knaust, R. Reinhardt, U. Neumann, et al., Transcriptome analysis of enriched *Golovinomyces orontii* haustoria by deep 454 pyrosequencing, Fungal Genet. Biol. 49 (6) (2012) 470–482.

[27] L. Jones, S. Riaz, A. Morales-Cruz, K.C.H. Amrine, B. McGuire, W.D. Gubler, et al., Adaptive genomic structural variation in the grape powdery mildew pathogen, *Erysiphe necator*, BMC Genomics. 15 (1) (2014) 1081.

[28] D. Vela-Corcía, R. Bautista, A. De Vicente, P.D. Spanu, A. Pérez-García, *De novo* analysis of the epiphytic transcriptome of the cucurbit powdery mildew fungus *Podosphaera xanthii* and identification of candidate secreted effector proteins, PLoS One 11 (10) (2016) 1–21.

[29] G. Sharma, R. Amenidi, D. Saxena, A. Gupta, P. Banerjee, D. Jain, et al., Effector mining from the *Erysiphe pisi* haustorial transcriptome identifies novel candidates involved in pea powdery mildew pathogenesis, Mol. Plant Pathol. 20 (2019) 1506–1522.

[30] D. Foster-Hartnett, D. Danesh, S. Peñuela, N. Sharopova, G. Endre, K.A. Vandenbosch, et al., Molecular and cytological responses of *Medicago truncatula* to *Erysiphe pisi*, Mol. Plant Pathol. 8 (3) (2007) 307–319.

[31] D.A. Samac, S. Peñuela, J.A. Schnurr, E.N. Hunt, D. Foster-Hartnett, K.A. Vandenbosch, et al., Expression of coordinately regulated defence response genes and analysis of their role in disease resistance in *Medicago truncatula*, Mol. Plant Pathol. 12 (8) (2011) 786–798.

[32] M. Curto, F. Krajinski, H. Küster, D. Rubiales, Plant defense responses in *Medicago truncatula* unveiled by microarray analysis, Plant Mol. Biol. Report. (2014) 569–583.

[33] A.J. Westermann, S.A. Gorski, J. Vogel, Dual RNA-seq of pathogen and host, Nat. Rev. Microbiol 10 (9) (2012) 618–630. Available from https://doi.org/10.1038/nrmicro2852.

[34] Y. Kawahara, Y. Oono, H. Kanamori, T. Matsumoto, T. Itoh, E. Minami, Simultaneous RNA-seq analysis of a mixed transcriptome of rice and blast fungus interaction, PLoS One 7 (11) (2012) 1–15.

[35] S. Asai, G. Rallapalli, S.J.M. Piquerez, M.C. Caillaud, O.J. Furzer, N. Ishaque, et al., Expression profiling during *Arabidopsis*/downy mildew interactionr a highly-expressed effector that attenuates responses to salicylic acid, PLoS Pathog. 10 (10) (2014) e1004443.

[36] F.E. Meyer, L.S. Shuey, S. Naidoo, T. Mamni, D.K. Berger, A.A. Myburg, et al., Dual RNA-sequencing of *Eucalyptus nitens* during *Phytophthora cinnamomi* challenge reveals pathogen and host factors influencing compatibility, Front. Plant Sci. 7 (2016) 1–15. Available from: https://doi.org/10.3389/fpls.2016.00191/abstract.

[37] A.S. Petitot, A. Dereeper, M. Agbessi, C. Da Silva, J. Guy, M. Ardisson, et al., Dual RNA-seq reveals *Meloidogyne graminicola* transcriptome and candidate effectors during the interaction with rice plants, Mol. Plant Pathol. 17 (6) (2016) 860–874.

[38] D. Banyal, Diversity analysis of *Erysiphe pisi* populations causing pea powdery mildew in Himachal Pradesh, Ind. Phytopathol. 67 (3) (2014) 263–267.

[39] D. Chandran, Y.C. Tai, G. Hather, J. Dewdney, C. Denoux, D.G. Burgess, et al., Temporal global expression data reveal known and novel salicylate-impacted processes and regulators mediating powdery mildew growth and reproduction on *Arabidopsis*, Plant Physiol 149 (3) (2009) 1435–1451. Available from https://doi.org/10.1104/pp.108.132985.

[40] J. Vogel, S. Somerville, Isolation and characterization of powdery mildew-resistant *Arabidopsis* mutants, Proc. Natl. Acad. Sci. 97 (4) (2000) 1897–1902. Available from: https://doi.org/10.1073/pnas.030531997.

[41] R.K. Patel, M. Jain, NGS QC toolkit: a toolkit for quality control of next generation

sequencing data, PLoS One 7 (2) (2012) e30619.
[42] C. Trapnell, L. Pachter, S.L. Salzberg, TopHat: discovering splice junctions with RNA-Seq, Bioinformatics. 25 (9) (2009) 1105–1111.
[43] B.J. Haas, A. Papanicolaou, M. Yassour, M. Grabherr, P.D. Blood, J. Bowden, et al., De novo transcript sequence reconstruction from RNA-seq using the trinity platform for reference generation and analysis, Nat. Protoc. 8 (8) (2013) 1494–1512.
[44] K.G. Bankar, V.N. Todur, R.N. Shukla, M. Vasudevan, Ameliorated *de novo* transcriptome assembly using Illumina paired end sequence data with trinity assembler, Genomics Data 5 (2015) 352–359. Available from https://doi.org/10.1016/j.gdata.2015.07.012.
[45] B. Li, C.N. Dewey, RSEM: accurate transcript quantification from RNA-Seq data with or without a reference genome, BMC Bioinform. 12 (2011) 323.
[46] B. Langmead, S.L. Salzberg, Fast gapped-read alignment with Bowtie 2, Nat. Methods 9 (4) (2012) 357–359.
[47] U. Ligges, M. Machler, Scatterplot3d –an R package for visualizing multivariate data, J. Stat. Softw. (2003) 1–20.
[48] S.F. Altschul, W. Gish, W. Miller, E.W. Myers, D.J. Lipman, Basic local alignment search tool, J. Mol. Biol. 215 (3) (1990) 403–410.
[49] M.I. Love, W. Huber, S. Anders, Moderated estimation of fold change and dispersion for RNA-seq data with DESeq2, Genome Biol. 15 (12) (2014) 1–21.
[50] J. Kim, H. Bang, Three common misuses of P values, Dent Hypoth. 7 (3) (2016) 73–80.
[51] O. Thimm, O. Bla, Y. Gibon, A. Nagel, S. Meyer, P. Kru, et al., MAPMAN : a user-driven tool to display genomics data sets onto diagrams of metabolic pathways and other biological processes, Plant J. (2004) 914–939.
[52] F. Supek, M. Bošnjak, N. Škunca, T. Šmuc, Revigo summarizes and visualizes long lists of gene ontology terms, PLoS One 6 (7) (2011) e21800.
[53] J. Jin, F. Tian, D.C. Yang, Y.Q. Meng, L. Kong, J. Luo, et al., PlantTFDB 4.0: toward a central hub for transcription factors and regulatory interactions in plants, Nucleic Acids Res. 45 (D1) (2017) D1040–D1045.
[54] K. Higo, Y. Ugawa, M. Iwamoto, T. Korenaga, Plant cis-acting regulatory DNA elements (PLACE) database, Nucleic Acid Res. 27 (1) (1999) 297–300.
[55] A. Conesa, S. Götz, J.M. García-Gómez, J. Terol, M. Talón, M. Robles, Blast2GO: a universal tool for annotation, visualization and analysis in functional genomics research, Bioinformatics. 21 (18) (2005) 3674–3676.
[56] J.D. Bendtsen, H. Nielsen, G. Von Heijne, S. Brunak, Improved prediction of signal peptides: SignalP 3.0, J. Mol. Biol. 340 (4) (2004) 783–795.
[57] T.N. Petersen, S. Brunak, G. von Heijne, H. Nielsen, SignalP 4.0: discriminating signal peptides from transmembrane regions, Nat. Methods 8 (10) (2011) 785–786. Available from: https://doi.org/10.1038/nmeth.1701.
[58] O. Emanuelsson, S. Brunak, G. von Heijne, H. Nielsen, Locating proteins in the cell using TargetP, SignalP and related tools, Nat. Protoc. 2 (4) (2007) 953–971.
[59] A. Krogh, B. Larsson, G. Von Heijne, E.L.L. Sonnhammer, Predicting transmembrane protein topology with a hidden Markov model: application to complete genomes, J. Mol. Biol. 305 (3) (2001) 567–580.
[60] B. Eisenhaber, G. Schneider, M. Wildpaner, F. Eisenhaber, A sensitive predictor for potential GPI lipid modification sites in fungal protein sequences and its application to genome-wide studies for *Aspergillus nidulans*, *Candida albicans*, *Neurospora crassa*, *Saccharomyces cerevisiae* and *Schizosaccharomyces pombe*, J. Mol. Biol. 337 (2) (2004) 243–253.
[61] J. Sperschneider, P.N. Dodds, K.B. Singh, J.M. Taylor, ApoplastP: prediction of effectors and plant proteins in the apoplast using machine learning, New Phytol. 217 (4) (2018) 1764–1778.
[62] J. Sperschneider, A.M. Catanzariti, K. Deboer, B. Petre, D.M. Gardiner, K.B. Singh, et al., LOCALIZER: subcellular localization prediction of both plant and effector proteins in the plant cell, Sci. Rep 7 (2017) 1–14. Available from https://doi.org/10.1038/srep44598.
[63] J.M. Ruijter, C. Ramakers, H. WMH, Y. Karlen, O. Bakker, van den hoff MJB, et al., Amplification efficiency: linking baseline and bias in the analysis of quantitative PCR data, Nucleic Acids Res 37 (6) (2009) e45.
[64] I.E. Maldonado-Mendoza, G.R. Dewbre, M.L. van Buuren, W.K. Versaw, M.J. Harrison, Methods to estimate the proportion of plant and fungal RNA in an arbuscular mycorrhiza, Mycorrhiza. 12 (2002) 67–74.
[65] T.D. Schmittgen, K.J. Livak, Analyzing real-time PCR data by the comparative CTmethod, Nat. Protoc. 3 (6) (2008) 1101–1108.
[66] C. Heath, Hypersensitive response-related death, Plant Mol. Biol. (2000) 321–334.
[67] M. Fernández-aparicio, E. Prats, A.A. Emeran, D. Rubiales, Characterization of resistance mechanisms to powdery mildew (*Erysiphe betae*) in beet (*Beta vulgaris*), Phytopathology 99 (4) (2009) 385–389.
[68] R. Mittler, Oxidative stress, antioxidants and stress tolerance, Trends Plant Sci. 7 (9) (2002) 405–410.
[69] Y. Yamauchi, A. Hasegawa, A. Taninaka, M. Mizutani, Y. Sugimoto, NADPH-dependent reductases involved in the detoxification of reactive carbonyls in plants, J. Biol. Chem. 286 (9) (2011) 6999–7009.
[70] P. Guo, Z. Li, P. Huang, B. Li, S. Fang, J. Chu, et al., A tripartite amplification loop involving the transcription factor WRKY75, salicylic acid, and reactive oxygen species accelerates leaf senescence, Plant Cell 29 (11) (2017) 2854–2870.
[71] J. Li, G. Brader, T. Kariola, P.E. Tapio, WRKY70 modulates the selection of signaling pathways in plant defense, Plant J. (2006) 477–491.
[72] R.M.F. Hussain, A.H. Sheikh, I. Haider, M. Quareshy, *Arabidopsis* WRKY50 and TGA transcription factors synergistically activate expression of PR1, Front. Plant Sci. 9 (7) (2018) 1–16.
[73] Q. Gao, S. Venugopal, D. Navarre, A. Kachroo, Low oleic acid-derived repression of jasmonic acid-inducible defense responses requires the WRKY50 and WRKY51 proteins, Plant Physiol. 155 (1) (2011) 464–476.
[74] Z. Zheng, S.A. Qamar, Z. Chen, T. Mengiste, *Arabidopsis* WRKY33 transcription factor is required for resistance to necrotrophic fungal pathogens, Plant J. 48 (4) (2006) 592–605.
[75] S.P. Pandey, M. Roccaro, M. Schön, E. Logemann, I.E. Somssich, Transcriptional reprogramming regulated by WRKY18 and WRKY40 facilitates powdery mildew infection of *Arabidopsis*, Plant J. 64 (6) (2010) 912–923.
[76] O. Lorenzo, R. Piqueras, J.J. Sánchez-serrano, R. Solano, ETHYLENE RESPONSE FACTOR 1 integrates signals from ethylene and jasmonate pathways in plant defense, Plant Cell 15 (1) (2003) 165–178.
[77] M. Pre, M. Atallah, A. Champion, M. De Vos, M.J. Pieterse, J. Memelink, The AP2/ERF domain transcription factor ORA59 integrates jasmonic acid and ethylene signals in plant defense, Plant Physiol. 147 (7) (2008) 1347–1357.
[78] C.S. Moffat, R.A. Ingle, D.L. Wathugala, N.J. Saunders, H. Knight, M.R. Knight, ERF5 and ERF6 play redundant roles as positive regulators of JA/Et-mediated defense against *Botrytis cinerea* in *Arabidopsis*, PLoS One 7 (4) (2012) e35995.
[79] F.Y. Cao, T.A. Defalco, W. Moeder, B. Li, Y. Gong, X. Liu, et al., *Arabidopsis* ETHYLENE RESPONSE FACTOR 8 (ERF8) has dual functions in ABA signaling and immunity, BMC Plant Biol. 8 (2018) 1–16.
[80] S. Chu, J. Wang, Y. Zhu, S. Liu, X. Zhou, H. Zhang, et al., An R2R3-type MYB transcription factor, GmMYB29, regulates isoflavone biosynthesis in soybean, PLoS Genet. 13 (5) (2017) 1–26.
[81] J. Takeda, Y. Ito, K. Maeda, Y. Ozeki, Assignment of UVB-responsive cis-element and protoplastization-(dilution-) and elicitor-responsive ones in the promoter region of a carrot phenylalanine ammonia-lyase gene (gDcPAL1), Photochem. Photobiol 76 (2) (2002) 232–238. Available from http://www.ncbi.nlm.nih.gov/pubmed/12194222.
[82] H. Shi, G. Liu, Y. Wei, Z. Chan, The zinc-finger transcription factor ZAT6 is essential for hydrogen peroxide induction of anthocyanin synthesis in *Arabidopsis*, Plant Mol. Biol 97 (1) (2018) 165–176. Available from https://doi.org/10.1007/s11103-018-0730-0.
[83] M. Qureshi, S. Neerakkal, The zinc finger protein ZAT11 modulates paraquat-induced programmed cell death in *Arabidopsis thaliana*, Acta Physiol. Plant. (2013) 1863–1871.
[84] Q. Bu, H. Jiang, C. Li, Q. Zhai, J. Zhang, X. Wu, et al., Role of the *Arabidopsis thaliana* NAC transcription factors ANAC019 and ANAC055 in regulating jasmonic acid-signaled defense responses, Cell Res. 18 (7) (2008) 756–767.
[85] J.H. Kim, J. Park, J. Kim, J. Ju, S. Hong, J. Kim, et al., Time-evolving genetic networks reveal a NAC troika that negatively regulates leaf senescence in *Arabidopsis*, Proc. Natl. Acad. Sci. 115 (21) (2018) E4930–E4939.
[86] H. Tsukagoshi, W. Busch, P.N. Benfey, Transcriptional regulation of ROS controls transition from proliferation to differentiation in the root, Cell 143 (4) (2010) 606–616. Available from https://doi.org/10.1016/j.cell.2010.10.020.
[87] C. Schuster, C. Gaillochet, A. Medzihradszky, W. Busch, G. Daum, M. Krebs, et al., A regulatory framework for shoot stem cell control integrating metabolic, transcriptional, and phytohormone signals, Dev. Cell 28 (4) (2014) 438–449. Available from https://doi.org/10.1016/j.devcel.2014.01.013.
[88] Y. Liu, X. Li, K. Li, H. Liu, C. Lin, Multiple bHLH proteins form heterodimers to mediate CRY2-dependent regulation of flowering-time in *Arabidopsis*, PLoS Genet. 9 (10) (2013) e1003861.
[89] K. Kazan, J.M. Manners, MYC2: the master in action, Mol. Plant 6 (3) (2013) 686–703. Available from https://doi.org/10.1093/mp/sss128.
[90] D. Godfrey, H. Böhlenius, C. Pedersen, Z. Zhang, J. Emmersen, H. Thordal-Christensen, Powdery mildew fungal effector candidates share N-terminal Y/F/WxC-motif, BMC Genomics 11 (1) (2010) 317.
[91] S. Bhattacharjee, C.M. Garner, W. Gassmann, New clues in the nucleus: transcriptional reprogramming in effector-triggered immunity, Front. Plant Sci. 4 (9) (2013) 1–7. Available from: https://doi.org/10.3389/fpls.2013.00364/abstract.
[92] H. Cui, K. Tsuda, J.E. Parker, Effector-triggered immunity: from pathogen perception to robust defense, Annu. Rev. Plant Biol. 66 (1) (2015) 487–511. Available from: https://doi.org/10.1146/annurev-arplant-050213-040012.
[93] A. Brutus, F. Sicilia, A. Macone, F. Cervone, G. De Lorenzo, A domain swap approach reveals a role of the plant wall-associated kinase 1 (WAK1) as a receptor of oligogalacturonides, Proc. Natl. Acad. Sci. 107 (20) (2010) 9452–9457. Available from: https://doi.org/10.1073/pnas.1000675107.
[94] J.S. Thaler, P.T. Humphrey, N.K. Whiteman, Evolution of jasmonate and salicylate signal crosstalk, Trends Plant Sci 17 (5) (2012) 260–270. Available from https://doi.org/10.1016/j.tplants.2012.02.010.
[95] L. Liu, F. Sonbol, B. Huot, Y. Gu, J. Withers, M. Mwimba, et al., Salicylic acid receptors activate jasmonic acid signalling through a non-canonical pathway to promote effector-triggered immunity, Nat. Commun 7 (2016) 13099. Available from https://doi.org/10.1038/ncomms13099.
[96] F. Zhu, D. Xi, S. Yuan, F. Xu, D. Zhang, H. Lin, Salicylic acid and jasmonic acid are essential for systemic resistance against tobacco mosaic virus in *Nicotiana benthamiana*, Mol. Plant-Microbe Interact. 27 (6) (2014) 567–577.
[97] K. Tsuda, M. Sato, T. Stoddard, J. Glazebrook, F. Katagiri, Network properties of robust immunity in plants, PLoS Genet. 5 (12) (2009) e1000772.
[98] B. Huot, J. Yao, B.L. Montgomery, S.Y. He, Growth-defense tradeoffs in plants: a balancing act to optimize fitness, Mol. Plant 7 (8) (2014) 1267–1287.
[99] T.L. Karasov, E. Chae, J.J. Herman, J. Bergelson, Mechanisms to mitigate the trade-off between growth and defense, Plant Cell 29 (4) (2017) 666–680. Available from: doi/10.1105/tpc.16.00931.
[100] D. Chandran, N. Inada, G. Hather, C.K. Kleindt, M.C. Wildermuth, Laser microdissection of *Arabidopsis* cells at the powdery mildew infection site reveals site-specific processes and regulators, Proc. Natl. Acad. Sci. 107 (1) (2010) 460–465. Available from: https://doi.org/10.1073/pnas.0912492107.
[101] K.M. Pajerowska-Mukhtar, W. Wang, Y. Tada, N. Oka, L. Chandra, J.P. Fonseca, et al., The HSF-like transcription factor TBF1 is a major molecular switch for plant

growth-to-defense transition, Curr. Biol. 22 (2) (2012) 103–112.
[102] R. Volz, S. Kim, J. Mi, K.G.M. Id, X. Guo, J.B. Id, et al., The Trihelix transcription factor GT2-like 1 (GTL1) promotes salicylic acid metabolism, and regulates bacterial-triggered immunity, PLoS Genet. 14 (10) (2018) e1007708.
[103] J.A. Lopez, Y. Sun, P.B. Blair, M.S. Mukhtar, TCP three-way handshake: linking developmental processes with plant immunity, Trends Plant Sci 20 (4) (2015) 238–245. Available from https://doi.org/10.1016/j.tplants.2015.01.005.
[104] S.H. Kim, G.H. Son, S. Bhattacharjee, H.J. Kim, J.C. Nam, P.D.T. Nguyen, et al., The *Arabidopsis* immune adaptor SRFR1 interacts with TCP transcription factors that redundantly contribute to effector-triggered immunity, Plant J. 78 (6) (2014) 978–989.
[105] M. Li, H. Chen, J. Chen, M. Chang, I.A. Palmer, W. Gassmann, et al., TCP transcription factors interact with NPR1 and contribute redundantly to systemic acquired resistance, Front. Plant Sci. 9 (8) (2018) 1–12. Available from: https://doi.org/10.3389/fpls.2018.01153/full.
[106] N. Zhang, Z. Wang, Z. Bao, L. Yang, D. Wu, X. Shu, et al., MOS1 functions closely with TCP transcription factors to modulate immunity and cell cycle in *Arabidopsis*, Plant J. 93 (1) (2018) 66–78.
[107] M. Trujillo, K. Shirasu, Ubiquitination in plant immunity, Curr. Opin. Plant Biol 13 (4) (2010) 402–408. Available from https://doi.org/10.1016/j.pbi.2010.04.002.
[108] M. Trujillo, K. Ichimura, C. Casais, K. Shirasu, Negative regulation of PAMP-triggered immunity by an E3 ubiquitin ligase triplet in *Arabidopsis*, Curr. Biol. 18 (18) (2008) 1396–1401.
[109] H. Häweker, S. Rips, H. Koiwa, S. Salomon, Y. Saijo, D. Chinchilla, et al., Pattern recognition receptors require N-glycosylation to mediate plant immunity, J. Biol. Chem. 285 (7) (2010) 4629–4636.
[110] J. Withers, X. Dong, Post-translational regulation of plant immunity, Curr. Opin. Plant Biol 38 (2017) 124–132. Available from https://doi.org/10.1016/j.pbi.2017.05.004.
[111] K. Pajerowska-mukhtar, X. Dong, A kiss of death — proteasome-mediated membrane fusion and programmed cell death in plant defense against bacterial infection, Genes Dev. 23 (21) (2009) 2449–2454.
[112] J. Chowdhury, M. Henderson, P. Schweizer, R.A. Burton, G.B. Fincher, A. Little, Differential accumulation of callose, arabinoxylan and cellulose in nonpenetrated versus penetrated papillae on leaves of barley infected with *Blumeria graminis* f. sp. *hordei*, New Phytol. 204 (3) (2014) 650–660.
[113] L. Tan, S. Eberhard, S. Pattathil, C. Warder, J. Glushka, C. Yuan, et al., An *Arabidopsis* cell wall proteoglycan consists of pectin and arabinoxylan covalently linked to an arabinogalactan protein, Plant Cell 25 (1) (2013) 270–287.
[114] S. Shailasree, K.R. Kini, S. Deepak, B.S. Kumudini, H.S. Shetty, Accumulation of hydroxyproline-rich glycoproteins in pearl millet seedlings in response to *Sclerospora graminicola* infection, Plant Sci. 167 (6) (2004) 1227–1234.
[115] S. Naidoo, E.A. Visser, L. Zwart, Y. du Toit, V. Bhadauria, L.S. Shuey, Dual RNA-sequencing to elucidate the plant-pathogen duel, Curr. Issues Mol. Biol. 27 (2018) 127–142. Available from: https://www.caister.com/cimb/abstracts/v27/127.html.
[116] C. Pedersen, E.V.L. van Themaat, L.J. McGuffin, J.C. Abbott, T.A. Burgis, G. Barton, et al., Structure and evolution of barley powdery mildew effector candidates, BMC Genomics 13 (1) (2012) 694.
[117] M.N. Grell, P. Mouritzen, H. Giese, A *Blumeria graminis* gene family encoding proteins with a C-terminal variable region with homologues in pathogenic fungi, Gene. 311 (1–2) (2003) 181–192.
[118] C. Xue, Two novel fungal virulence genes specifically expressed in appressoria of the rice blast fungus, Plant Cell 14 (9) (2002) 2107–2119. Available from: https://doi.org/10.1105/tpc.003426.
[119] Y. Cao, X. Zhu, R. Jiao, Y. Xia, The *Magas1* gene is involved in pathogenesis by affecting penetration in *Metarhizium acridum*, J. Microbiol. Biotechnol. 22 (7) (2012) 889–893.
[120] R. Weßling, P. Epple, S. Altmann, Y. He, L. Yang, R. Henz, et al., Convergent targeting of a common host protein-network by pathogen effectors from three kingdoms of life, Cell Host Microbe 16 (3) (2015) 364–375.
[121] S. Kamoun, A catalogue of the effector secretome of plant pathogenic oomycetes, Annu. Rev. Phytopathol. 44 (2006) 41–60.
[122] P. Krishnan, X. Ma, B.A. Mcdonald, P.C. Brunner, Widespread signatures of selection for secreted peptidases in a fungal plant pathogen, BMC Evol. Biol. 18 (1) (2018) 7.
[123] Y. Xia, Proteases in pathogenesis and plant defence, Cell. Microbiol. 6 (10) (2004) 905–913.
[124] C. Schoina, N.V. Kruif, F. Grovers, K. Bouwmeester, Clade 5 aspartic proteases of *Phytophthora infestans* are virulence factors implied in RXLR effector cleavage, Eur. J. Plant Pathol. 154 (1) (2019) 17–29.
[125] D. Bui, Y. Lee, J.Y. Lim, M. Fu, J. Kim, G.J. Choi, et al., Heat shock protein 90 is required for sexual and asexual development, virulence, and heat shock response in *Fusarium graminearum*, Sci. Rep 6 (2016) 28154. Available from https://doi.org/10.1038/srep28154.